Mathematical Biology



Front propagation in the shadow wave-pinning model

Daniel Gomez¹ • King-Yeung Lam² · Yoichiro Mori¹

Received: 5 August 2022 / Revised: 8 February 2023 / Accepted: 22 March 2023 /

Published online: 10 April 2023

© The Author(s), under exclusive licence to Springer-Verlag GmbH Germany, part of Springer Nature 2023

Abstract

In this paper we consider a non-local bistable reaction—diffusion equation which is a simplified version of the wave-pinning model of cell polarization. In the small diffusion limit, a typical solution u(x,t) of this model approaches one of the stable states of the bistable nonlinearity in different parts of the spatial domain Ω , separated by an interface moving at a normal velocity regulated by the integral $\int_{\Omega} u(x,t) \, dx$. In what is often referred to as wave-pinning, feedback between mass-conservation and bistablity causes the interface to slow and approach a fixed limit. In the limit of a small diffusivity $\varepsilon^2 \ll 1$, we prove that for any $0 < \gamma < 1/2$ the interface can be estimated within $O(\varepsilon^\gamma)$ of the location as predicted using formal asymptotics. We also discuss the sharpness of our result by comparing the formal asymptotic results with numerical simulations.

Mathematics Subject Classification $35K57 \cdot 35B25 \cdot 35B40 \cdot 35B30$

1 Introduction

Scalar reaction—diffusion equations and systems can be useful in the modeling of phase transition in various physical and biological systems. Of particular interest is the case of bistable reaction diffusion equations for which (Fife and McLeod 1977) provided one of the first rigorous treatments. The problem has since received considerable attention in higher dimensions such as, for example, the analysis of generation and dynamics of interfaces using comparison principle methods by Chen (1992) and the analysis of

☑ Daniel Gomez d1gomez@sas.upenn.edu

> King-Yeung Lam lam.184@math.ohio-state.edu

Yoichiro Mori y1mori@sas.upenn.edu

- Department of Mathematics, University of Pennsylvania, Philadelphia, PA 19104-6395, USA
- Department of Mathematics, The Ohio State University, Columbus, OH 43210-1174, USA



72 Page 2 of 31 D. Gomez et al.

interface motion using level set and viscosity solution methods by Barles et al. (1992, 1993). Generalizations of these classical bistable reaction—diffusion equations that, for example, incorporate non-local effects or replace the single reaction—diffusion equation with a system, are also known to exhibit phase transition phenomenon (Rubinstein and Sternberg 1992; Chen et al. 2010; Cusseddu et al. 2019), though their rigorous analysis is considerably less studied. For example, the formal analysis by Rubinstein and Sternberg (1992), as well as the subsequent rigorous analysis by Chen et al. (2010), illustrates that travelling front solutions to certain non-local scalar reaction—diffusion systems can exhibit many similarities to their classical, local, counterparts.

In this paper we initiate a rigorous treatment of a non-local bistable reactiondiffusion equation as an analytically tractable model of cell polarization (Mori et al. 2008, 2011). This model distills the complex biochemical circuitry leading to the polarization of Rho GTPases to a two-species mass-conserved reaction-diffusion system for the concentration of active and inactive GTPases. A delicate interplay between bistability and mass conservation in this system can lead to the expansion and eventual halting of an activated GTPase patch, a phenomenon which is commonly referred to as wave-pinning. The relative simplicity of this two-species model, together with its analytical tractability and the interpretability of its results, has made it an attractive framework for cell-polarization models. More recent iterations of the wave-pinning model have incorporated mechanochemical feedback (Zmurchok et al. 2020) and bulksurface coupling (Rätz and Röger 2012; Diegmiller et al. 2018; Cusseddu et al. 2019). Within the context of bulk-surface coupling Giese et. al. have also probed the effects of diffusion barriers and cell shape (Giese et al. 2015). We remark that alternative models for cell-polarization specifically and cellular pattern formation in general have also been proposed and this is an active area of research. See, e.g. the review articles (Jilkine and Edelstein-Keshet 2011; Goryachev and Leda 2017; Rappel and Edelstein-Keshet 2017; Champneys et al. 2021).

In this paper we consider specifically the non-local reaction—diffusion equation

$$\begin{cases} u_{t}(x,t) = \varepsilon \Delta u(x,t) + \varepsilon^{-1} f(u(x,t),v(t)), & x \in \Omega, \quad t > 0, \quad (1.1a) \\ v(t) = M_{0} - \frac{1}{|\Omega|} \int_{\Omega} u(x,t) dx, & t > 0, \quad (1.1b) \\ \partial_{n} u(x,t) = 0, & x \in \partial \Omega, \quad t > 0, \quad (1.1c) \\ u(x,0) = u_{0}(x), & x \in \Omega, \quad (1.1d) \end{cases}$$

where $\Omega \subset \mathbb{R}^N$ $(N \geq 1)$ is a bounded domain with smooth boundary, $M_0 > 0$, $\varepsilon > 0$ are constants, and f(u,v) is a smooth function which is bistable in u with additional properties to be made more precise below. The well-posedness of solution to (1.1) is discussed in Sect. 1.1 below. This non-local equation is formally obtained by taking the limit $D \to \infty$, often referred to as the *shadow limit*, in the mass-conserved reaction–diffusion system

$$\begin{cases} u_t = \varepsilon \Delta u + \varepsilon^{-1} f(u, v), & \varepsilon v_t = D \Delta v - f(u, v), & x \in \Omega, & t > 0, \\ \partial_n u = \partial_n v = 0, & x \in \partial \Omega, & t > 0, \\ u(x, 0) = u_0(x), & v(x, 0) = v_0(x), & x \in \Omega, & t = 0. \end{cases}$$



Specifically, assuming $D \gg 1$ we then consider the asymptotic expansion $v(x,t) \sim v_0(x,t) + \cdots$ from which we deduce the leading order expression $\Delta v_0 = 0$. Together with the homogeneous Neumann boundary conditions this implies that $v_0(x,t)$ is spatially constant. Moreover, mass conservation

$$\frac{d}{dt} \int_{\Omega} (u(x,t) + v(x,t)) dx = 0,$$

then implies that v=v(t) where v(t) is given by (1.1b). The analysis of wave-pinning in these systems by Mori et al. (2011), as well as of its subsequent iterations (e.g. Cusseddu et al. 2019; Zmurchok et al. 2020), primarily rely on numerical simulations and the use of formal asymptotic methods in the sharp interface limit for which $\varepsilon \ll 1$. Our goal in this paper is to initiate a rigorous treatment of front solutions to (1.1) by rigorously demonstrating that such solutions converge to those obtained using formal asymptotics as $\varepsilon \to 0^+$.

The remainder of this paper is organized as follows. We begin by first recalling in Sect. 1.2 some preliminary properties of travelling front solutions in \mathbb{R}^1 due to Fife and McLeod (1977). After making precise assumptions about the initial condition $u_0(x)$ in Sect. 1.3 we will then state in Sect. 1.4 the leading order solution to (1.1) obtained using formal asymptotic methods and describe in more detail the conditions for wave-pinning to arise. This is accompanied with an illustrative example in Sect. 1.5 for which we numerically simulate (1.1). In Sect. 1.6 we precisely state our assumptions on the reaction-kinetics f(u, v) and state our main result in Theorem 2. In Sect. 2 we prove convergence results for the scalar counterpart of (1.1) where v is a prescribed function, which is subsequently used in the proof of Theorem 2 in Sect. 3.

Before proceeding further, we describe the most important assumptions on the reaction kinetics f(u, v) in order to establish some common notations. The first assumption we make is that for a range of $v \in [v_{\min}, v_{\max}]$ the function f(u, v) is bistable in u. Specifically this means that $f(\cdot, v)$ has exactly three zeros $h^-(v) < h^0(v) < h^+(v)$ such that

$$f_u(h^{\pm}(v), v) < 0$$
 and $f_u(h^0(v), v) > 0$. (1.2)

These inequalities imply in particular that $h^\pm(v)$ (resp. $h^0(v)$) are stable (resp. unstable) with respect to the reaction kinetics. In addition we assume that the spatially homogeneous steady states $(u,v)=(h^\pm(v_0^\pm),v_0^\pm)$, where v_0^\pm is obtained by substituting $u=h^\pm(v_0^\pm)$ into (1.1b), noting that $|\Omega|=1$, and solving the resulting nonlinear equation $v_0^\pm+h^\pm(v_0^\pm)=M_0$, are linearly stable. We can derive an algebraic relation for linear stability by letting $u=h^\pm(v_0^\pm)+\phi_j(x)e^{\lambda t}$ where ϕ_j is the eigenfunction satisfying $-\Delta\phi_j=\mu_j\phi_j$ in Ω and $\partial_n\phi_j=0$ on $\partial\Omega$. Since $\mu_0=0$ and $\phi_0=1$ whereas $\mu_j>0$ and $\int_\Omega\phi_jdx=0$ for all remaining $j\geq 1$, substituting into (1.1a) and linearizing yields two cases

$$\begin{cases} \lambda = \varepsilon^{-1} (f_u(h^{\pm}(v_0^{\pm}), v_0^{\pm}) - f_v(h^{\pm}(v_0^{\pm}), v_0^{\pm})), & j = 0, \\ \lambda = -\mu_j + \varepsilon^{-1} f_u(h^{\pm}(v_0^{\pm}), v_0^{\pm}), & j \ge 1. \end{cases}$$



Page 4 of 31 D. Gomez et al.

When $j \ge 1$ we immediately deduce that $\lambda < 0$ by the bistability of $f(\cdot, v)$ whereas for i = 0 we deduce the linear stability condition

$$f_u(h^{\pm}(v_0^{\pm}), v_0^{\pm}) - f_v(h^{\pm}(v_0^{\pm}), v_0^{\pm}) < 0.$$
 (1.3)

1.1 Existence and uniqueness result

Note that (1.1) can be rewritten into the following single, nonlocal parabolic equation

Note that (1.1) can be rewritten into the following single, nonlocal parabolic equation
$$\begin{cases} u_t(x,t) = \varepsilon \Delta u(x,t) + \varepsilon^{-1} f(u(x,t), M_0 - \frac{1}{|\Omega|} \int_{\Omega} u(x,t) dx), & x \in \Omega, \quad t > 0, \\ \partial_n u(x,t) = 0, & x \in \partial \Omega, \quad t > 0, \\ u(x,0) = u_0(x), & x \in \Omega. \end{cases}$$
(1.4b)

Since the integral term $\int_{\Omega} u \, dx$ has better regularity than u, one can apply the usual semigroup argument to obtain existence and uniqueness of classical solution.

Theorem 1 For each nonnegative $u_0 \in C(\overline{\Omega})$, (1.4) has a unique classical solution $u \in C(\overline{\Omega} \times [0, \infty)) \cap C^{2,1}(\overline{\Omega} \times (0, \infty)).$

Proof Set $X = C(\overline{\Omega})$ and

$$\begin{cases} D(-\Delta) = \left\{ \phi \in \bigcap_{p>1} W^{2,p}(\Omega) : \Delta \phi \in C(\overline{\Omega}), \ \partial_n \phi \big|_{\partial \Omega} = 0 \right\}, \\ X_{1/2} = \left\{ \phi \in C^1(\overline{\Omega}) : \ \partial_n \phi \big|_{\partial \Omega} = 0 \right\} \end{cases}$$

The existence and uniqueness of a classical solution in the class

$$C([0, T_{\text{max}}); X) \cap C^{1}((0, T_{\text{max}}); X) \cap C((0, T_{\text{max}}); D(-\Delta))$$

defined on some maximal time interval $[0, T_{\text{max}})$ is a consequence of semigroup theory (Lunardi 1995, Theorem 7.1.5 and Proposition 7.1.10); See also (Lam and Lou 2022, Theorem 5.1.2). Next, observe that $T_{\text{max}} = +\infty$ since the solution remains bounded for all time thanks to the bistable nonlinearity f. Finally, by observing that u, and the nonlinearity $f\left(u, M_0 - \frac{1}{|\Omega|} \int_{\Omega} u \, dx\right)$ belongs to $C^{\beta, \beta/2}(\overline{\Omega} \times [\delta, \frac{1}{\delta}])$ for every $0 < \delta < 1$, it follows from the Schauder estimates that $u \in C^{2,1}(\overline{\Omega} \times [\delta, 1/\delta])$ for each $0 < \delta < 1$.

1.2 Travelling front solutions in \mathbb{R}^1

Let $v \in (v_{\min}, v_{\max})$ and assume that $a \in \mathbb{R}$ is sufficiently small so that f(u, v) - a is bistable. Denote by $h^0(v; a)$ and $h^{\pm}(v; a)$ the unstable and stable zeros of $f(\cdot, v) - a$



respectively. It can then be shown that (see Fife and McLeod 1977 for example)

$$q_{rr} + \alpha q_r + f(q, v) - a = 0, \quad -\infty < r < \infty, \tag{1.5a}$$

$$q(0, v; a) = h^{0}(v; a), \quad q(r, v; a) \to h^{\mp}(v; a), \quad r \to \pm \infty, \quad (1.5b)$$

can be solved for a unique front profile q(r, v; a) and front speed $\alpha(v; a)$. Moreover, it can be shown that q(r, v; a) is monotone decreasing in r so that multiplying (1.5a) by q_r and integrating yields the explicit expression for the front speed

$$\alpha(v;a) = \frac{1}{\int_{-\infty}^{\infty} |q_r(r,v;a)|^2 dr} \int_{h^-(v;a)}^{h^+(v;a)} (f(u,v) - a) du.$$
 (1.6)

In addition to these properties we also have the following ordering property for the front speed under the additional assumption that $\partial f/\partial v \ge 0$.

Lemma 1.1 Let $v_{\min} < v_1 < v_2 < v_{\max}$ and $a \in \mathbb{R}$ be such that both $f(\cdot, v_1) - a$ and $f(\cdot, v_2) - a$ are bistable. If $\partial f/\partial v \ge 0$ then $\alpha(v_1; a) \le \alpha(v_2; a)$.

Proof First, we assume in addition that $\partial f/\partial v > 0$. Let $q_i(r) \equiv q(r, v_i; a)$ and $\alpha_i \equiv \alpha(v_i; a)$ for each i = 1, 2. Observe that $\partial f/\partial v > 0$ implies that $h^{\pm}(v_1; a) < h^{\pm}(v_2; a)$. Since q is strictly decreasing in r and $q(\pm \infty; v_2; a) > q(\pm \infty; v_1; a)$, we can perform a translation to find values r_1 and r_2 such that

$$q_1(r_1) = q_2(r_2), \quad q_1'(r_1) = q_2'(r_2), \quad q_1''(r_1) \le q_2''(r_2).$$

From (1.5a) we then obtain

$$q_2''(r_2) - q_1''(r_1) + (\alpha_2 - \alpha_1)q_1'(r_1) = f(q_1(r_1), v_1) - f(q_2(r_2), v_2) \le 0, (1.7)$$

which implies $\alpha_2 - \alpha_1 > 0$.

For the general case $\partial f/\partial v \ge 0$, choose $\delta > 0$ small and repeat the above arguments to $f + \delta v$, and then let $\delta \to 0$.

Remark 1.1 By differentiating $f(h^{\pm}(v;a),v)-a=0$ with respect to a we readily deduce that $\frac{dh^{\pm}}{da}<0$. On the other hand we similarly calculate $\frac{dh^0}{da}>0$.

Remark 1.2 The a-dependent reaction kinetics f(u, v) - a are important for the convergence proof in Sect. 2; see also (Barles et al. 1993). When a = 0 we will write $\alpha(v)$, $h^0(v)$, and $h^{\pm}(v)$ instead of $\alpha(v; 0)$, $h^0(v; 0)$, and $h^{\pm}(v; 0)$ respectively.

1.3 Well-prepared initial conditions

By replacing x, t, ε with $x/|\Omega|^{1/N}$, $t/|\Omega|^{1/N}$, and $\varepsilon/|\Omega|^{1/N}$, respectively, we may assume without loss of generality that Ω is of unit volume, e.g. $|\Omega| = 1$. We will be making this assumption for the remainder of the paper.



Throughout this paper we will also assume that the initial condition $u_0(x)$ is well-prepared in the following sense. We fix $\Omega_0 \subset \Omega$ and define the initial interface $\Gamma_0 = \partial \Omega_0 \setminus \partial \Omega$ which we assume to be a Lipschitz surface intersecting $\partial \Omega$ transversally. More precisely, we assume that there exists a constant $\mathcal{M}_0 > 1$ such that the following two conditions hold:

(L) For each $x_0 \in \Gamma_0$ there exists a neighborhood $\mathcal{N} \subset \overline{\Omega}$ of x_0 such that the surface $\Gamma_0 \cap \mathcal{N}$ can be represented as the graph of a Lipschitz function. Specifically, up to an orthogonal change of coordinates

$$\Gamma_0 \cap \mathcal{N} = \{ (x', x_N) \in \mathcal{N}' \times \mathbb{R} \mid x_N = G_{x_0}(x') \},$$

where $G_{x_0}: \mathcal{N}' \subset \mathbb{R}^{N-1} \to \mathbb{R}$ satisfies $|G_{x_0}(x) - G_{x_0}(y)| \leq \mathcal{M}_0|x - y|$ for all $x, y \in \mathcal{N}'$.

(T) For each $x_0 \in \Gamma_0 \cap \partial \Omega$, using the same local coordinates as above, we have

$$|n_{\partial\Omega}(x_0)\cdot(0,\cdots,0,1)^T|\leq \mathcal{M}_0^{-1},$$

where $n_{\partial\Omega}(x_0)$ denotes the outer unit normal vector of $\partial\Omega$ at the point x_0 . Note that (T) holds trivially if $\Gamma_0 \cap \partial\Omega$ is empty.

Next we let v_0 solve the algebraic equation

$$v_0 + |\Omega_0|h^+(v_0) + (1 - |\Omega_0|)h^-(v_0) = M_0,$$
 (1.8a)

where we assume that Ω_0 and M_0 are chosen in such a way that (1.8a) has a solution in $v_0 \in (v_{\min}, v_{\max})$. In terms of this value of v_0 and the geometric constraints on Ω_0 we then define the initial condition $u_0(x)$ by

$$u_0(x) = \begin{cases} h^+(v_0), & x \in \Omega_0, \\ h^-(v_0), & x \in \Omega \setminus \Omega_0. \end{cases}$$
 (1.8b)

Remark 1.3 With this choice of well-prepared initial conditions we bypass the question of front generation and focus instead exclusively on front propagation.

Remark 1.4 The geometric constraints on the initial interface Γ_0 are needed for the proofs of Theorems 2 and 3. If Γ_0 is a smooth surface, then we only need

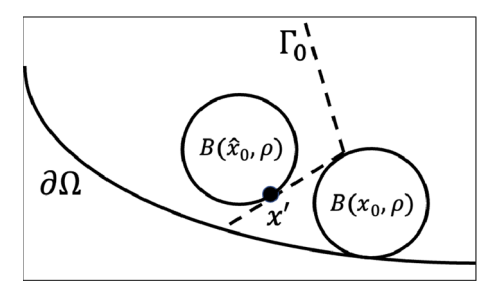
$$|n_{\partial\Omega}(x_0)\cdot n_{\Gamma_0}|<1\quad\text{for all }x_0\in\Gamma_0\cap\partial\Omega,$$

where n_{Γ_0} is the normal vector with respect to Γ_0 .

We state, without proof, the following consequence of the geometric constraints on Ω_0 and Γ_0 (see Fig. 1 for an illustration).



Fig. 1 Illustration of Lemma 1.2. The sets $\partial\Omega$ and Γ_0 are represented by the solid and dash curves respectively. For given $x' \in \Gamma_0$ and $\rho > 0$, the choice of $B(x_0, \rho)$ and $B(\hat{x}_0, \rho)$ are displayed



Lemma 1.2 Let $\Omega_0 \subset \Omega$ and its boundary $\Gamma_0 = \partial \Omega$ satisfy the geometric constraints (L) and (T) above. Then there exist $\underline{\rho} > 0$ and $\overline{K}_0 > 1$ such that for any $x' \in \Gamma_0$ and $\rho \in (0, \rho]$, there exists $x_0 \in \Omega_0$, $\hat{x}_0 \in \Omega \setminus \overline{\Omega}_0$ such that

$$B(x_0, \rho) \subset \Omega_0$$
, $B(\hat{x}_0, \rho) \subset \Omega \backslash \Omega_0$,

and

$$|x' - x_0| + |x' - \hat{x}_0| \le \bar{K}_0 \rho.$$

Here $B(x_0, \rho_0) = \{x \in \mathbb{R}^N \mid |x - x_0| < \rho_0\}$ and \bar{K}_0 only depends on $\partial \Omega$ and the constant \mathcal{M}_0 .

1.4 Leading order solution and wave-pinning

Using the method of matched asymptotic expansions we can formally derive a leadingorder approximation of solutions to (1.1) under the assumptions of a well-prepared initial condition. We first state the following definition of a signed distance function which we will use throughout the remainder of paper.

Definition 1 Let $S \subset \mathbb{R}^N$ be arbitrary. The signed distance from $\partial S = \overline{S} \cap \overline{\Omega \backslash S}$ is then defined by

$$\operatorname{dist}(x, \partial S) = \begin{cases} \inf_{y \in \partial S} |x - y|, & x \in \Omega \backslash S, \\ -\inf_{y \in \partial S} |x - y|, & x \in S. \end{cases}$$
 (1.9)

Let $\Gamma_0 = \partial \Omega_0$ be the interface described in Sect. 1.3. For each t, we define the domain $\hat{\Omega}(t)$ and value $\hat{v}(t)$ by solving the system

$$\begin{cases}
\hat{\Omega}(t) \equiv \left\{ x \in \Omega \mid \text{dist}(x, \Gamma_0) < \int_0^t \alpha(\hat{v}(\tau)) d\tau \right\}, \\
\hat{v}(t) = M_0 - |\hat{\Omega}(t)| h^+(\hat{v}(t)) - \left(1 - |\hat{\Omega}(t)|\right) h^-(\hat{v}(t)),
\end{cases} (1.10a)$$

where $\alpha(\cdot)$ is the front-speed given by (1.6) with a=0. Note that $\hat{\Omega}(0)=\Omega_0$.

Equations (1.10a) and (1.10b) together constitute a differential algebraic equation (DAE) which can in general be solved for $\hat{v}(t)$ and $\hat{\Omega}(t)$ uniquely. We refer the reader



72 Page 8 of 31 D. Gomez et al.

to Appendix A for a reformulation of this DAE which more readily lends itself to numerical calculation. Note that $\hat{v}(0) = v_0$ coincides with the value of v_0 chosen in Sect. 1.3 above. The leading order asymptotic approximation for u^{ε} when $\varepsilon \ll 1$ is then given in terms of $\hat{\Omega}(t)$ and $\hat{v}(t)$ by

$$\hat{u}(x,t) = h^{+}(\hat{v}(t))\chi_{\hat{\Omega}(t)}(x) + h^{-}(\hat{v}(t))\chi_{\Omega\setminus\hat{\Omega}(t)}(x), \tag{1.10c}$$

where $\chi_S(x)$ is the indicator function for any $S \subset \mathbb{R}^N$.

Remark 1.5 If v(t) is prescribed independently of u in (1.1) then one can define $\hat{\Omega}(t)$ by (1.10a) and the same leading-order solution (1.10c) can be obtained; see Sect. 2.

The formal construction of the approximation (1.10) relies solely on the bistability of the reaction kinetics and the well-preparedness of the initial condition. If we assume in addition that $\alpha'(v) \geq 0$ and the existence of a $v_c \in (v_{\min}, v_{\max})$ such that $\alpha(v_c) = 0$, then solutions to (1.1) may exhibit wave-pinning (WP) in which the front slows and approaches a fixed interface. The possibility of this behaviour is readily seen by differentiating (1.10b) with respect to t to get

$$\frac{d\hat{v}}{dt} = -\frac{h^{+}(\hat{v}(t)) - h^{-}(\hat{v}(t))}{1 + |\hat{\Omega}(t)| \frac{dh^{+}}{dv}|_{\hat{v}(t)} + (1 - |\hat{\Omega}(t)|) \frac{dh^{-}}{dv}|_{\hat{v}(t)}} |\partial \hat{\Omega}(t) \backslash \partial \Omega |\alpha(\hat{v}(t)).$$

$$\tag{1.11}$$

Observe that the denominator is strictly positive as a consequence of the linear stability of the homogeneous steady states. Indeed, by differentiating the identity $f(h^{\pm}(v), v) = 0$ with respect to v and using the stability condition (1.3), we obtain

$$0 = f_u(h^{\pm}(v), v) \frac{dh^{\pm}}{dv} + f_v(h^{\pm}(v), v) > f_u(h^{\pm}(v), v) \left(\frac{dh^{\pm}}{dv} + 1\right).$$
 (1.12)

In view of (1.2), it follows that $dh^{\pm}/dv > -1$.

By (1.11), we deduce that $d\hat{v}/dt$ is negatively proportional to the front speed which in particular implies that $d\hat{v}/dt \leq 0$ for $\hat{v}(t) \geq v_c$ and this suggests three distinct outcomes for the dynamics of the leading order solutions to (1.1): (I) $\hat{\Omega}(t) \to \emptyset$ in finite time, (II) $\hat{\Omega}(t) \to \Omega$ in finite time, or (III) $\alpha(\hat{v}(t)) \to 0$ and $\hat{\Omega}(t) \to \Omega_{\infty} \subset \Omega$ as $t \to \infty$. The particular outcome depends on the properties of the well-prepared initial condition and, ignoring boundary effects, can be heuristically classified solely by the values $|\Omega_0|$ and M_0 . To do so, we start by defining

$$M(v, w) = v + wh^{+}(v) + (1 - w)h^{-}(v)$$
 for $v \in [v_{\min}, v_{\max}], w \in [0, 1],$

$$(1.13)$$

in terms of which (1.10b) is equivalent to $M(\hat{v}(t), |\hat{\Omega}(t)|) = M_0$. Next, we calculate

$$\frac{\partial M}{\partial v} = 1 + w \frac{dh^+}{dv} + (1 - w) \frac{dh^-}{dv}, \quad \frac{\partial M}{\partial w} = h^+(v) - h^-(v),$$



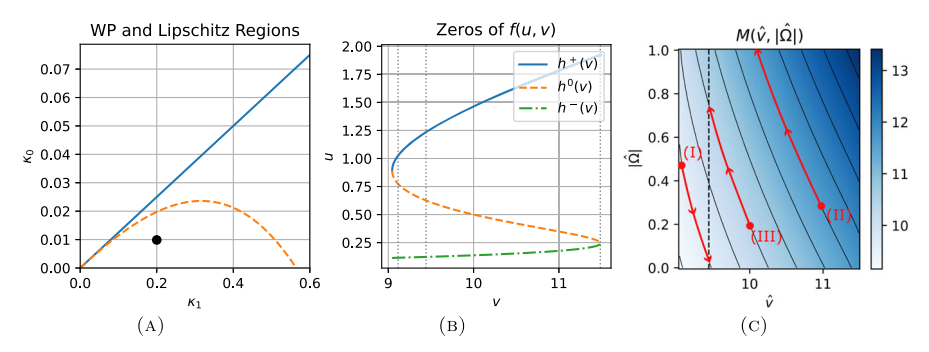


Fig. 2 A Plot of the wave-pinning threshold (solid blue) for the nonlinearity specified in (1.14). wave-pinning is formally known to occur for values of κ_0 and κ_1 below the solid blue curve. The rigorous results in this paper are restricted to choices of κ_0 and κ_1 below the dashed orange curve. The dot indicates the values of $\kappa_1 = 0.2$ and $\kappa_0 = 0.01$ used in **B** and **C** and for the simulations in the example of Sect. 1.5. **B** Zeros $h^-(v)$, $h^0(v)$, and $h^+(v)$ of (1.14). **C** Color plot of $M(\hat{v}, |\hat{\Omega}|)$ showing trajectories of the leading order solution (1.10) along its contours with each label coinciding with the possible outcomes of Proposition 1.1 (colour figure online)

both of which we observe to be positive. Since the dynamics of $|\hat{\Omega}(t)|$ and $\hat{v}(t)$ are restricted to the contours $M(\hat{v}(t), \hat{\Omega}(t)) = M_0$ we can immediately deduce a criteria for each outcome (I), (II), and (III) based on whether $v_0 < v_c$ or $v_0 > v_c$ and whether the contour intersects $|\hat{\Omega}| = 0$ or $|\hat{\Omega}| = 1$ (see Fig. 2c for an example). We summarize this classification in the following proposition.

Proposition 1.1 The dynamics of the leading order solution (1.10) have the following three outcomes depending on the parameters v_0 and $|\Omega_0|$ and are determined by the value of $M(v_0, |\Omega_0|)$ defined by (1.13):

- (I) if $v_{\min} + h^-(v_{\min}) < M(v_0, |\Omega_0|) < v_c + h^-(v_c)$ then $\hat{\Omega}(t) \to \emptyset$ in finite time,
- (II) if $v_c + h^+(v_c) < M(v_0, |\Omega_0|) < v_{\text{max}} + h^+(v_{\text{max}})$ then $\hat{\Omega}(t) \to \Omega$ in finite time, and

(III) if
$$v_c + h^-(v_c) < M(v_0, |\Omega_0|) < v_c + h^+(v_c)$$
 then $\alpha(\hat{v}(t)) \to 0$ and $\hat{\Omega}(t) \to \Omega_\infty \subset \Omega$ as $t \to \infty$.

Note that in Case (III) above it is possible that $\Omega_{\infty} = \emptyset$ or $\Omega_{\infty} = \Omega$, but the convergence is not achieved in finite time. In particular, regardless of the outcome in the above proposition we deduce the following properties of $\hat{v}(t)$ and $\alpha(\hat{v}(t))$.

Lemma 1.3 Let $\hat{v}(t)$ solve (1.10a) and (1.10b) where Γ_0 satisfies the geometric assumptions in Sect. 1.3 and $\hat{v}(0) = v_0 \in (v_{\min}, v_{\max})$. Then $v_{\min} < \hat{v}(t) < v_{\max}$ and $\alpha(\hat{v}(t))$ is of one sign for all $t \geq 0$.

1.5 Example

In this subsection, we illustrate the wave-pinning phenomenon in a two-dimensional domain by numerically simulating (1.1) using the finite element method software Flex-PDE7 (http://www.pdesolutions.com). Throughout our simulations we let the reaction



72 Page 10 of 31 D. Gomez et al.

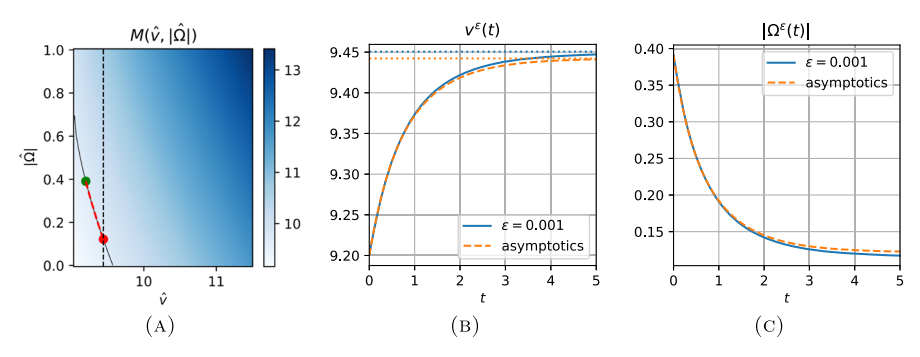


Fig. 3 Comparison of numerical and leading order asymptotic solutions. Parameter values used found in the main body. A Numerically computed trajectory $(v_{\text{num}}(t), |\Omega_{\text{num}}(t)|)$ (dashed red) superimposed on a colorplot of $M(\hat{v}, |\hat{\Omega}|)$. B Comparison of $v_{\text{num}}(t)$ (solid blue curve) and $\hat{v}(t)$ (dashed orange curve). The horizontal orange dotted line indicates the value of $v_c = \hat{v}(+\infty)$ (note that $v_c = \hat{v}(+\infty)$ and $|\hat{\Omega}(\infty)|$ are uniquely determined by (1.10b)). The horizontal blue dotted line indicates the $O(\varepsilon)$ corrected v_c^ε after taking the mean curvature dynamics into account and determined by solving by $\alpha(v_c^\varepsilon) = \varepsilon R_c^{-1}$, where $\pi R_c^2 = |\hat{\Omega}(\infty)|$. C Comparison of $|\Omega_{\text{num}}(t)|$ (solid blue) and $|\hat{\Omega}(t)|$ (dashed orange) (colour figure online)

kinetics be of the commonly used form

$$f(u, v) = \left(\kappa_0 + \frac{\kappa_1 u^2}{1 + u^2}\right) v - u. \tag{1.14}$$

These reaction kinetics are known to satisfy the conditions for wave-pinning provided that $\kappa_0 < \kappa_1/8$ (Mori et al. 2011). Our proof of Theorem 2 applies in the more restrictive parameter regime indicated in Fig. 2a needed to satisfy assumption (1.16) below. This region was numerically computed by enforcing that $|dh^\pm/dv| < 1$ at $v = v_c$ which guarantees the existence of a neighborhood (v_{\min}, v_{\max}) of v_c for which, in addition to the bistability condition, assumption (1.16) holds. Fixing $\kappa_1 = 0.2$ and $\kappa_0 = 0.01$ we can then calculate $h^\pm(v)$ and $h^0(v)$ which we plot in Fig. 2b together with the numerically calculated values $v_c \approx 9.4422$, $v_{\min} \approx 9.1151$, and $v_{\max} \approx 11.486$. In Fig. 2c we plot $M(v_0, |\Omega_0|)$ together with the critical value v_c (dashed vertical line) and three sample trajectories of $|\hat{\Omega}(t)|$ versus $\hat{v}(t)$ labelled according to the three possible outcomes (I), (II), and (III) in Proposition 1.1.

To demonstrate the wave-pinning mechanism, and the accuracy of the leading order solution (1.10), we consider an illustrative example for which we numerically solve (1.1) using FlexPDE7 (http://www.pdesolutions.com) with $\varepsilon=0.001$ and $\Omega\subset\mathbb{R}^2$ being a disk of unit area centred at the origin. We use (1.8b) as the initial condition where Ω_0 is an ellipse centered at the origin with major- and minor-axis lengths of a=0.50777 and b=0.24520 respectively. Choosing $M_0=9.7$ then gives a value of $v_0\approx 9.2$ which is less than v_c so that the leading-order theory predicts that v^ε will increase toward v_c and the area of the activated region will decrease. In Fig. 3a we indicate by a green and red dot the, respectively, initial and final (obtained by the formal leading order theory) values of v^ε and the volume of the activated region. We henceforth denote the numerically computed solution by $u_{\text{num}}(x,y,t)$ and $v_{\text{num}}(t)$ in terms of which we define the numerical activated region by



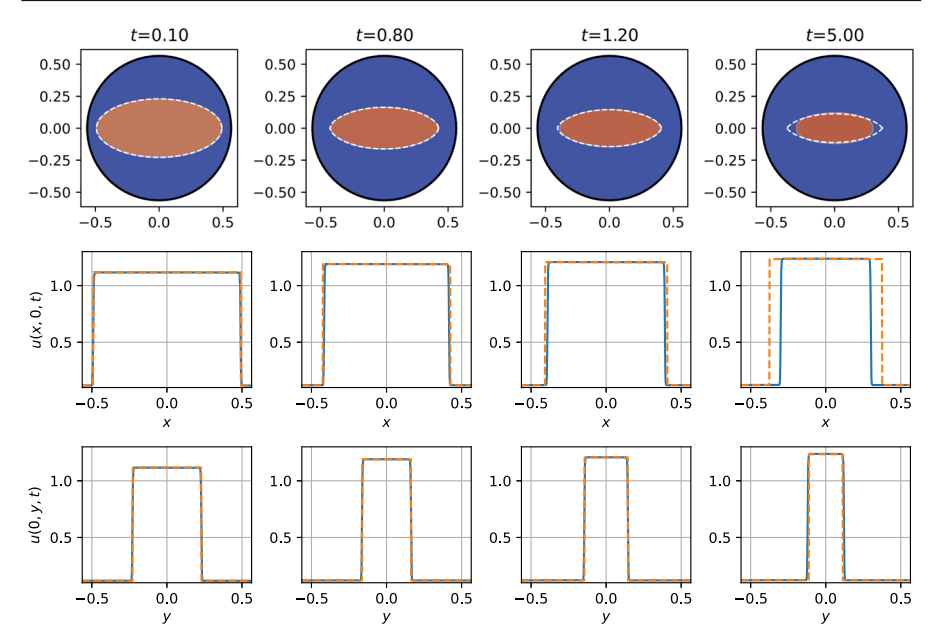


Fig. 4 Comparison of the numerically calculated solution $u_{\text{num}}(x, y, t)$ and the leading order asymptotic theory. The top row shows a colorplot of $u_{\text{num}}(x, y, t)$ with the leading order trajectory superimposed as the dashed white curve. In the middle and bottom rows we plot cross sections of $u_{\text{num}}(x, y, t)$ (solid blue) and $\hat{u}(x, y, t)$ (dashed orange) along y = 0 (middle) and x = 0 (bottom). The time of each snapshot and cross section is indicated at the top of each column (colour figure online)

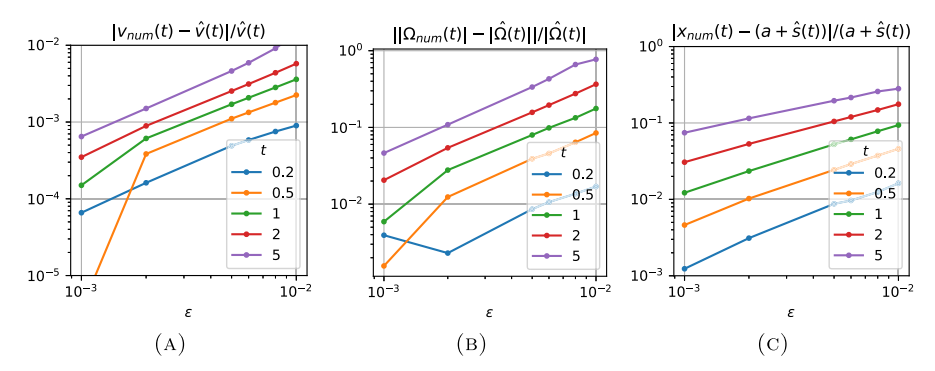


Fig. 5 Relative error between the numerically computed solution and the leading order asymptotic theory

$$\Omega_{\mathrm{num}}(t) = \bigg\{ (x,y) \in \Omega \, \bigg| \, u_{\mathrm{num}}(x,y,t) > \tfrac{1}{2} \left(\max_{(x,y) \in \Omega} u_{\mathrm{num}}(x,y,t) + \min_{(x,y) \in \Omega} u_{\mathrm{num}}(x,y,t) \right) \bigg\}.$$

The numerically calculated values of $v_{\text{num}}(t)$ and $|\Omega_{\text{num}}(t)|$ thus obtained are indicated by the dashed red curve in Fig. 3a which shows good agreement with the expected behaviour of the leading order solution in that it follows a contour of $M(\hat{v}, |\hat{\Omega}|)$. Similarly, we compare $v_{\text{num}}(t)$ and $|\Omega_{\text{num}}(t)|$ to their leading order counterparts in Fig. 3b, c respectively. In the top row of Fig. 4 we plot, at the indicated values of



t, a colorplot of the numerically computed solution $u_{\text{num}}(x, y, t)$ with the leading order trajectory of the front superimposed and indicated by the dashed white line. The remaining rows of Fig. 4 show cross sections of u_{num} (solid blue) and \hat{u} (dashed orange) along y = 0 (middle row) and x = 0 (bottom row). Finally, in Fig. 6 we show the evolution of the activated region over a longer timescale which suggests the front evolves according to a volume-conserved mean curvature flow (Fig. 5).

While Figs. 3 and 4 show good qualitative agreement between the numerically computed solution and the leading order asymptotic theory, there are some clear quantitative discrepancies. Although subtle, we first note that there appears to be a slight mismatch when comparing the numerical and leading order asymptotic solutions in Fig. 3b, c. This discrepancy is due to higher-order corrections to the leading-order asymptotic theory which we expect to be of order $O(\varepsilon)$. Indeed, based on numerical experiments (see Fig. 6) as well as past results on travelling front solutions to bistable reaction-diffusion systems (e.g. Rubinstein and Sternberg 1992; Barles et al. 1993), we expect that as $v^{\varepsilon}(t)$ approaches its limiting value, the front will undergo a volume-conserved mean curvature flow over a slower timescale. As a consequence, we anticipate that the mismatch observed in Fig. 3 is of order ε and sufficient to counteract the tendency of the mean curvature flow to shrink the activated region further. An approximation to the corrected limiting value of $v^{\varepsilon}(t)$ can be obtained by first noting that, to leading order, the limiting volume of the activated region can be found by substituting $\hat{v}(t) = v_c$ into (1.10b) and solving for $|\hat{\Omega}(\infty)| = \lim_{t \to \infty} |\hat{\Omega}(t)|$. Since the subsequent volume-preserving mean-curvature flow ultimately leads to a ball of radius $R_c = (|\hat{\Omega}(\infty)|/\pi)^{1/2}$, we deduce $v_c^{\varepsilon} = \lim_{t\to\infty} v^{\varepsilon}(t)$ must solve $\alpha(v_c^{\varepsilon}) = \varepsilon R_c^{-1}$. In Fig. 3b we plotted both v_c (dotted orange) and v_c^{ε} (dotted blue) showing good agreement with the limiting behaviour of \hat{v} and v^{ε} respectively. Finally, in Fig. 5a, b we show the results of repeating our numerical calculations for additional values of $\varepsilon = 0.002, 0.005, 0.006, 0.008, 0.01$ to calculate the relative error with the leading order asymptotic theory. We observe that while the relative error increases for larger values of t, it still remains $O(\varepsilon)$. However, this is not the case for Fig. 5c.

In addition to the discrepancies in Fig. 3 discussed above, we also observe in Fig. 4 that when t=5 there is a mismatch between the numerical and leading-order asymptotic solutions near the extremities of the activated region along y=0. This mismatch is in part due to the higher-order mean curvature effects discussed above, though we expect this to play only a secondary role. Instead, we expect that this mismatch is primarily due to the formation of a cusp in the leading order front evolution which first occurs around t=2. Indeed, at points where such a cusp emerges the asymptotic solution obtained using the method of matched asymptotic expansions is no longer valid. This discrepancy is in fact captured in our main result of Theorem 2 for which the error to the leading-order asymptotic theory is proven to be $O(\varepsilon^{\gamma})$ for any $\gamma \in (0, 1/2)$. In Fig. 5c we plot the relative error between the numerically calculated location of the front along y=0 and the leading order location of the front given by $x=a+\hat{s}(t)$ where $\hat{s}(t)$ is the solution to (A.1). Interestingly, we observe from these plots that the relative error is of order ε for smaller values of t whereas it becomes sub-linear as t increases before becoming approximately of order $\sqrt{\varepsilon}$ at t=5.



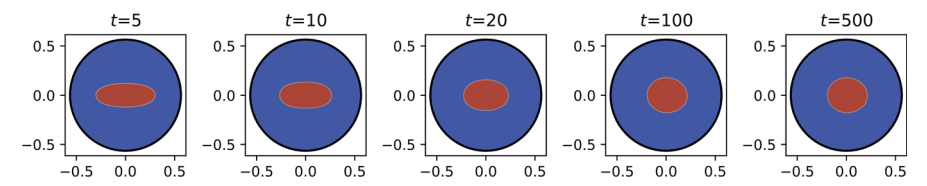


Fig. 6 Long time behaviour of the numerical solution considered in the example demonstrating volumepreserving mean curvature flow

1.6 The main result

The above example illustrates that the leading order approximation (1.10) is in good agreement with direct numerical simulations of (1.1). This example also suggests that for a fixed T>0, $\hat{v}(t)$ uniformly approximates $v^{\varepsilon}(t)$ in [0,T], while $\hat{u}(x,t)$ uniformly approximates $u^{\varepsilon}(x,t)$ away from the leading order front interface in $\overline{\Omega}\times[0,T]$. We make these observations rigorous in Theorem 2 which relies on the following four assumptions:

- (A1) There exists a pair $v_{\min} < v_{\max}$ such that for all $v \in [v_{\min}, v_{\max}]$ the nonlinearity $f(\cdot, v)$ is bistable with zeros $h^-(v) < h^0(v) < h^+(v)$ and such that the spatially homogeneous steady states $u = h^{\pm}(v)$ are linearly stable.
- (A2) There exists a unique value $v_c \in (v_{\min}, v_{\max})$ such that $\alpha(v_c) = 0$ where α is the front speed given by (1.6).
- (A3) The nonlinearity f(u, v) satisfies

$$\partial f/\partial v \ge 0$$
 for all u and $v \in [v_{\min}, v_{\max}].$ (1.15)

(A4) There exists a $\theta \in (0, 1)$ such that

$$|h^{\pm}(v_1) - h^{\pm}(v_2)| < (1 - \theta)|v_1 - v_2|$$
 for all $v \in [v_{\min}, v_{\max}]$. (1.16)

(A5) The domain Ω is convex.

Assumptions (A1)-(A3) are needed for wave-pinning to occur, though we note that (A3) can be weakened provided $\alpha(v_1) \leq \alpha(v_2)$ for all $v_1, v_2 \in (v_{\min}, v_{\max})$ with $v_1 \leq v_2$. On the other hand assumption (A4) is a technical assumption that is needed for the proof of Theorem 2. The convexity of Ω in assumption (A5) is introduced to simplify the treatment of boundary conditions in our construction of sub- and supersolutions in Sect. 2; see Remark 2.3. Finally we choose an A > 0 such that

$$\sup_{v_1, v_2 \in (v_{\min}, v_{\max})} |h^+(v_1) - h^-(v_2)| \le A \quad \text{and} \quad |\alpha(v_1) - \alpha(v_2)| \le A|v_1 - v_2|$$
(1.17)

for all $v_1, v_2 \in [v_{\min}, v_{\max}]$. Such an A exists due to the smoothness of h^{\pm} and α .

The following theorem is our main result and it provides quantitative estimates on the accuracy of the leading order solution constructed in (1.10).



Page 14 of 31 D. Gomez et al.

Theorem 2 Let f(u, v) satisfy assumptions (A1)–(A4), and let Ω satisfy assumption (A5). Suppose that the initial condition u_0 is given by (1.8b) such that the initial activated region Ω_0 satisfies the Lipschitz and transversality conditions (L) and (T) in Sect. 1.3. Then, for each T>0 and $\gamma\in(0,\frac{1}{2})$, there exists an $\varepsilon_1>0$ and $\bar{K}_1>0$ such that for all $\varepsilon \in (0, \varepsilon_1]$ and any solution $(\tilde{u}^{\varepsilon}(x, t), v^{\varepsilon})$ of (1.1), we have

$$\sup_{t\in[0,T]} |v^{\varepsilon}(t) - \hat{v}(t)| \le \bar{K}_1 \varepsilon^{\gamma},\tag{1.18a}$$

$$\sup_{t \in [0,T]} |v^{\varepsilon}(t) - \hat{v}(t)| \leq \bar{K}_{1} \varepsilon^{\gamma}, \tag{1.18a}$$

$$h^{-}(\hat{v}(t)) - \bar{K}_{1} \varepsilon^{\gamma} \leq u^{\varepsilon}(x,t) \leq h^{+}(\hat{v}(t)) + \bar{K}_{1} \varepsilon^{\gamma} \quad \text{in } \Omega \times [0,T], \tag{1.18b}$$

and

$$\begin{cases} |u^{\varepsilon}(x,t) - h^{+}(\hat{v}(t))| \leq \bar{K}_{1}\varepsilon^{\gamma} & \text{in } \{(x,t) \mid 0 \leq t \leq T, \text{ } \operatorname{dist}(x,\Gamma_{0}) < \int_{0}^{t} \alpha(\hat{v}(\tau)) d\tau - \bar{K}_{1}\varepsilon^{\gamma}\}, \\ |u^{\varepsilon}(x,t) - h^{-}(\hat{v}(t))| \leq \bar{K}_{1}\varepsilon^{\gamma} & \text{in } \{(x,t) \mid 0 \leq t \leq T, \text{ } \operatorname{dist}(x,\Gamma_{0}) > \int_{0}^{t} \alpha(\hat{v}(\tau)) d\tau + \bar{K}_{1}\varepsilon^{\gamma}\}, \\ |(1.19b)| & (1.19b) \end{cases}$$

where $\hat{v}(t)$ is given by (1.10b).

Note that above theorem treats the regime where the interface is driven by a constantin-space normal velocity modulated by the level of $v^{\varepsilon}(t)$. Such a regime takes place at a faster timescale then mean curvature and domain geometry effects. In this regime, the activated region at time t is defined by its distance to the initial interface Γ_0 . In particular, the initial activated region Ω_0 is not assumed to be connected. We prove Theorem 2 in Sect. 3 below. The proof relies crucially on the local convergence properties of appropriate sub- and super-solutions to a scalar counterpart of (1.1), which we analyze in Sect. 2 below.

2 Local convergence of a scalar PDE with time dependent nonlinearity

In this section we consider the following scalar counterpart to (1.1)

$$\begin{cases} \tilde{u}_t = \varepsilon \Delta \tilde{u} + \varepsilon^{-1} f(\tilde{u}, \tilde{v}(t)), & x \in \Omega, \quad t > 0, \\ \partial_n \tilde{u} = 0, & x \in \partial \Omega, \quad t > 0, \\ \tilde{u}(x, 0) = \tilde{u}_0(x), & x \in \Omega, \quad t = 0, \end{cases}$$
 (2.1a)

$$\partial_n \tilde{u} = 0, \qquad x \in \partial \Omega, \quad t > 0,$$
 (2.1b)

$$\tilde{u}(x,0) = \tilde{u}_0(x), \qquad x \in \Omega, \quad t = 0, \tag{2.1c}$$

where we assume that the nonlinearity f(u, v) satisfies the bistability assumption (A1) and where $\tilde{v}(t)$ is a prescribed function satisfying

$$\tilde{v} \in C^1([0,\infty))$$
 and $v_{\min} < \tilde{v}(t) < v_{\max}$ for all $t \ge 0$. (2.2a)

In addition we let $\Omega_0 \subset \Omega$ and its boundary $\Gamma_0 = \partial \Omega_0$ satisfy the geometric constraints (L) and (T) set forth in Sect. 1.3. We then assume that the initial condition $\tilde{u}_0(x)$ is



given by

$$\tilde{u}_0(x) = \begin{cases} h^+(\tilde{v}(0)), & x \in \Omega_0, \\ h^-(\tilde{v}(0)), & x \in \Omega \setminus \overline{\Omega}_0. \end{cases}$$
 (2.2b)

We are here interested in the limiting behaviour of solutions to (2.1) when $\varepsilon \ll 1$. To precisely state our main theorem for this section we first state the following definitions.

Definition 2 For a given $0 < \sigma < \frac{1}{2}$ and $\varepsilon > 0$ we define the following subsets of Ω

$$\tilde{\Omega}_{\varepsilon,\sigma}^{+}(t) \equiv \{ x \in \Omega \mid \operatorname{dist}(x, \Gamma_0) < \int_0^t \alpha(\tilde{v}(\tau)) d\tau - \varepsilon^{\sigma} \}, \tag{2.3}$$

$$\tilde{\Omega}_{\varepsilon,\sigma}^{-}(t) \equiv \{ x \in \Omega \mid \operatorname{dist}(x, \Gamma_0) > \int_0^t \alpha(\tilde{v}(\tau)) d\tau + \varepsilon^{\sigma} \}, \tag{2.4}$$

where dist (x, Γ_0) is the signed distance function so that dist $(x, \Gamma_0) < 0$ in Ω_0 .

Remark 2.1 Letting $\varepsilon \to 0$ in the definition of $\tilde{\Omega}_{\varepsilon,\sigma}^+(t)$ we obtain an analogue of the leading-order activated region $\hat{\Omega}(t)$ considered in Sect. 1.4. Indeed, the same asymptotic methods can be used to derive a leading order approximation of the form (1.10c) for (2.1). In this sense $\tilde{\Omega}_{\varepsilon,\sigma}^+(t)$ and $\tilde{\Omega}_{\varepsilon,\sigma}^-(t)$ are, respectively, subsets of the leading order activated and inactivated regions which closely (within $O(\varepsilon^{\sigma})$) approximate their leading order counterparts.

In terms of these definitions we have the following theorem whose proof will be the focus of the remainder of this section.

Theorem 3 Let T > 0, Ω a convex subset of \mathbb{R}^N with smooth boundary, and let $\Omega_0 \subset \Omega$ and assume that its boundary $\Gamma_0 \subset \partial \Omega_0$ satisfies the Lipschitz and transversality conditions (L) and (T) in Sect. 1.3. If $\tilde{u}^{\varepsilon}(x,t)$ satisfies (2.1) where $\tilde{v}(t)$ satisfies (2.2a) and the initial condition $\tilde{u}_0(x)$ is given by (2.2b), then for each $\sigma \in (0,\beta)$ and $\beta \in (0,1/2)$ there exists an $\varepsilon_2 > 0$ and $\bar{K}_2 > 0$ such that for all $\varepsilon \in (0,\varepsilon_2]$

$$\sup_{(x,t)\in\widehat{\Omega}_{\varepsilon,\sigma,T}^+} |\tilde{u}^{\varepsilon}(x,t) - h^+(\tilde{v}(t))| < \bar{K}_2 \varepsilon^{\beta}, \tag{2.5}$$

$$\sup_{(x,t)\in\tilde{\Omega}_{\varepsilon,\sigma,T}^{-}} |\tilde{u}^{\varepsilon}(x,t) - h^{-}(\tilde{v}(t))| < \bar{K}_{2}\varepsilon^{\beta}, \tag{2.6}$$

and

$$h^{-}(\tilde{v}(t)) - \bar{K}_{2}\varepsilon \le u^{\varepsilon}(x,t) \le h^{+}(\tilde{v}(t)) + \bar{K}_{2}\varepsilon \quad \text{for all } (x,t) \in \Omega \times [0,T].$$
(2.7)

Here $\tilde{\Omega}_{\varepsilon,\sigma,T}^{\pm}$ is given by

$$\tilde{\Omega}_{\varepsilon,\sigma,T}^{\pm} = \left\{ (x,t) \in \Omega \times [0,T] | x \in \tilde{\Omega}_{\varepsilon,\sigma}^{\pm}(t) \right\}. \tag{2.8}$$



72 Page 16 of 31 D. Gomez et al.

Remark 2.2 The bounds (2.5) and (2.6) in particular imply that for each $\sigma \in (0, 1/2)$ the interface of the activated region can be located within an error of $O(\varepsilon^{\sigma})$ from the limiting $\varepsilon \to 0$ problem.

Remark 2.3 The convexity assumption here is used in the verification of the subsolution. When the domain is convex, the spherically symmetric subsolution always has positive outward normal derivatives, thus satisfying differential inequality on the boundary. If the domain is nonconvex but is of class C^2 , then the same holds true provided the subsolution is supported on balls of sufficiently small radius. In such a case, one can possibly modify the arguments and remove the convexity assumption in this paper.

Our first lemma addresses the global bounds (2.7).

Lemma 2.1 Let T > 0 be given and suppose that \tilde{u}^{ε} satisfies (2.1) with assumptions (2.2). Then there exists an $\varepsilon_3 > 0$ and $\bar{K}_3 > 0$ such that for all $\varepsilon \in (0, \varepsilon_3]$

$$h^{-}(\tilde{v}(t)) - \bar{K}_{3}\varepsilon \le \tilde{u}^{\varepsilon}(x, t) \le h^{+}(\tilde{v}(t)) + \bar{K}_{3}\varepsilon \quad \text{for all } (x, t) \in \Omega \times [0, T].$$
(2.9)

Proof Let $g^-(t) = h^-(\tilde{v}(t)) - \bar{K}_3 \varepsilon$ and $g^+(t) = h^+(\tilde{v}(t)) + \bar{K}_3 \varepsilon$ where $\bar{K}_3 > 0$ is a large constant to be specified later. Since $f_u(h^\pm(\tilde{v}(t)), \tilde{v}(t)) < 0$ we can find $\gamma' > 0$ and $\varepsilon_3 > 0$ such that

$$f(g^+(t), \tilde{v}(t)) = f(g^+(t), \tilde{v}(t)) - f(h^+(\tilde{v}(t)), \tilde{v}(t)) \le -\gamma' \bar{K}_3 \varepsilon \quad \text{for } 0 \le t \le T, \quad \text{and } \varepsilon \in (0, \varepsilon_3].$$

Using the fact that $|\frac{dg^+}{dt}| = |\frac{\partial h^+}{\partial v} \frac{d\tilde{v}}{dt}|$ is uniformly bounded in ε we may specify $\bar{K}_3 > 0$ sufficiently large so that

$$\frac{dg^+}{dt} \ge \varepsilon^{-1} f(g^+, \tilde{v}),$$

and therefore $g^+(t)$ is a supersolution of (2.1). Since also $g^+(0) > h^+(\tilde{v}(0)) \ge \tilde{u}_0(x)$, we conclude by the maximum principle that $u^{\varepsilon}(x,t) \le g^+(t)$ for all $(x,t) \in \Omega \times [0,T]$. The proof of the lower bound $u^{\varepsilon}(x,t) \ge g^-(t)$ is similar and is omitted. \square

The proof of the bounds (2.5) is more intricate and we proceed by first constructing a class of radially symmetric sub- and super-solutions to (2.1).

Definition 3 For each $\delta > 0$ we define $\eta_{\delta}(z)$ to be the smooth real-valued function satisfying

$$\begin{cases} \eta_{\delta}(z) = z, & \text{for } z \ge -\delta/2, \\ -\delta \le \eta_{\delta}(z) \le -\delta/2, & \text{for } -\delta \le z \le -\delta/2, \\ \eta_{\delta}(z) = -\delta, & \text{for } z \le -\delta. \end{cases}$$
 (2.10)



72

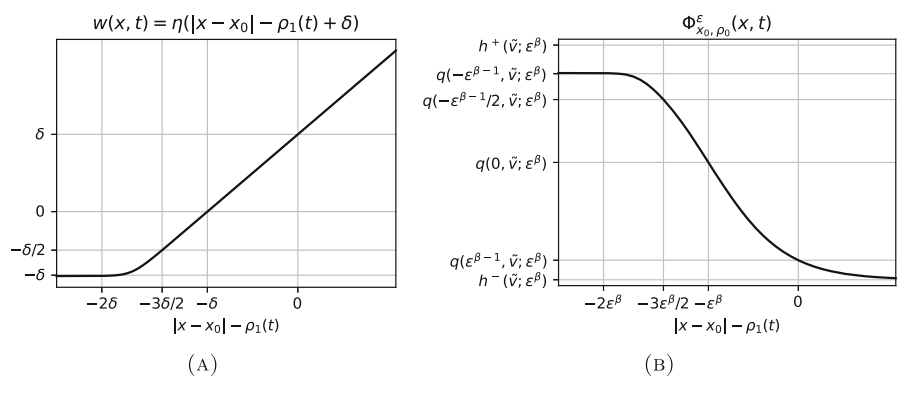


Fig. 7 Sketches of **A** the cut-off function w(x,t) defined by (2.10) and (2.13). **B** The sub-solution $\Phi_{\chi_0,\rho_0}^{\varepsilon}(x,t)$ from Lemma 2.2. We remind the reader that $\rho_1(t) \equiv \rho_0 + \int_0^t \alpha(\tilde{v}(\tau),\varepsilon^\beta) \,d\tau$

Definition 4 Let $\beta > 0$, $\rho_0 > 0$, T > 0, $\tilde{v} \in C^1([0, T])$, and $x_0 \in \Omega$ be given.

(1) Define T_{ε} , $\hat{T}_{\varepsilon} \in [0, T]$ by

$$T_{\varepsilon} = \sup \left\{ T' \in [0, T] \mid \rho_{0} + \int_{0}^{t} \alpha(\tilde{v}(\tau), \varepsilon^{\beta}) d\tau > 3\varepsilon^{\beta} \quad \text{for all } t \in [0, T'] \right\},$$

$$(2.11)$$

$$\hat{T}_{\varepsilon} = \sup \left\{ T' \in [0, T] \mid \rho_{0} - \int_{0}^{t} \alpha(\tilde{v}(\tau), -\varepsilon^{\beta}) d\tau > 3\varepsilon^{\beta} \quad \text{for all } t \in [0, T'] \right\},$$

where we set T_{ε} and \hat{T}_{ε} to zero if their corresponding sets are empty.

(2) Let $\delta = \varepsilon^{\beta}$ and define w(x, t) and $\hat{w}(x, t)$ by

$$w(x,t) = \eta_{\delta} \left(|x - x_{0}| - \rho_{0} - \int_{0}^{t} \alpha(\tilde{v}(\tau), \varepsilon^{\beta}) d\tau + \delta \right) \qquad \text{for } x \in \Omega, \ t \in [0, T_{\varepsilon}],$$

$$(2.13)$$

$$\hat{w}(x,t) = -\eta_{\delta} \left(|x - x_{0}| - \rho_{0} + \int_{0}^{t} \alpha(\tilde{v}(\tau), -\varepsilon^{\beta}) d\tau + \delta \right) \qquad \text{for } x \in \Omega, \ t \in [0, \hat{T}_{\varepsilon}].$$

$$(2.14)$$

(3) Define $\Phi_{x_0,\rho_0}^{\varepsilon}(x,t)$ and $\hat{\Phi}_{x_0,\rho_0}^{\varepsilon}(x,t)$ by

$$\Phi_{x_0,\rho_0}^{\varepsilon}(x,t) = q\left(\varepsilon^{-1}w(x,t), \tilde{v}(t); \varepsilon^{\beta}\right) \quad \text{for } (x,t) \in \Omega \times [0,T_{\varepsilon}], \quad (2.15)$$

$$\hat{\Phi}^{\varepsilon}_{x_0,\rho_0}(x,t) = q\left(\varepsilon^{-1}\hat{w}(x,t), \tilde{v}(t); -\varepsilon^{\beta}\right) \quad \text{for } (x,t) \in \Omega \times [0,\hat{T}_{\varepsilon}], \quad (2.16)$$

where q(r, v; a) is the travelling front profile satisfying (1.5).

A plot of the function w(x, t) is shown in Fig. 7a whereas Fig. 7b shows a sketch of $\Phi_{x_0, \rho_0}^{\varepsilon}$.



72 Page 18 of 31 D. Gomez et al.

Lemma 2.2 Let $\beta \in (0, 1/2)$, $\rho_0 > 0$, T > 0, $\tilde{v} \in C^1([0, T])$, and $x_0 \in \Omega$ be given. Then there exists an $\varepsilon_3 > 0$ such that for all $\varepsilon \in (0, \varepsilon_3]$ the function $\Phi^{\varepsilon}_{x_0, \rho_0}$ defined in (2.15) above satisfies

$$\begin{cases} \partial_{t} \Phi_{x_{0},\rho_{0}}^{\varepsilon} - \varepsilon \Delta \Phi_{x_{0},\rho_{0}}^{\varepsilon} - \varepsilon^{-1} f(\Phi_{x_{0},\rho_{0}}^{\varepsilon}, \tilde{v}(t)) \leq 0 & \text{in } \Omega \times [0, T_{\varepsilon}], \\ \partial_{n} \Phi_{x_{0},\rho_{0}}^{\varepsilon} \leq 0 & \text{on } \partial \Omega \times [0, T_{\varepsilon}]. \end{cases}$$

$$(2.17a)$$

Furthermore, the constant $\varepsilon_3 > 0$ depends on β but is independent of x_0 , ρ_0 .

Proof Obviously $\Phi_{x_0,\rho_0}^{\varepsilon}(x,t)$ is smooth in $\Omega\setminus\{x_0\}$. Moreover, the definition of T_{ε} and w(x,t) imply that $w(x,t) \equiv -\varepsilon^{\beta}$ in a neighborhood of x_0 so that in particular $\Phi_{x_0,\rho_0}^{\varepsilon}(x,t)$ is smooth for all $(x,t) \in \overline{\Omega} \times [0,T_{\varepsilon}]$.

From the well known properties of the front profile q (see for instance Fife and McLeod 1977) we can find an $r_0 > 0$ and v > 0 such that for all $v \in [v_{\min}, v_{\max}]$ and a in a neighborhood of zero,

$$|q_r(r, v; a)| + |q_{rr}(r, v; a)| < e^{-v|r|}$$
 for all $|r| > r_0$. (2.18)

For convenience, we also define the function

$$\rho_1(t) \equiv \rho_0 + \int_0^t \alpha(\tilde{v}(\tau), \varepsilon^{\beta}) d\tau, \qquad (2.19)$$

as well as the operator

$$\mathcal{L}[\phi] \equiv \partial_t \phi - \varepsilon \Delta \phi - \varepsilon^{-1} f(\phi, \tilde{v}(t)). \tag{2.20}$$

In terms of the radial coordinate $\rho(x) = |x - x_0|$ we directly calculate that

$$\mathcal{L}[\Phi_{x_0,\rho_0}^{\varepsilon}] = q_v \frac{d\tilde{v}}{dt} + \varepsilon^{-1} q_r \left[w_t - \varepsilon \left(w_{\rho\rho} + \frac{N-1}{\rho} w_{\rho} \right) + \alpha \right] + \varepsilon^{-1} q_{rr} \left(1 - |w_{\rho}|^2 \right) - \varepsilon^{\beta - 1}.$$
(2.21)

where $\alpha = \alpha(\tilde{v}(t); \varepsilon^{\beta})$ and that q and all its derivatives are evaluated at $(r, v; a) = (\varepsilon^{-1}w(x, t), \tilde{v}(t); \varepsilon^{\beta})$. We show (2.17a) by calculating the sign of the right-hand-side of (2.21) in three separate cases. Throughout the proof we use

$$\left|q_v \frac{d\tilde{v}}{dt}\right| + |q_r| + |q_{rr}| + |\alpha| \le C_0$$
 everywhere,

where C_0 is a generic constant that is independent of ε .

¹ By (A1), such an exponent v exist for each $v \in [v_{\min}, v_{\max}]$, and is the root of some quadratic equation. By continuity argument, v can be chosen uniformly in v.



Case 1. $\rho(x) - \rho_1(t) \ge -\frac{3}{2}\varepsilon^{\beta}$: In this case $w(x,t) = \rho(x) - \rho_1(t) + \varepsilon^{\beta}$ so that $w_t = -\alpha$, $w_{\rho} = 1$, $w_{\rho\rho} = 0$, and therefore

$$\mathcal{L}[\Phi_{x_0,\rho_0}^{\varepsilon}] = q_v \frac{d\tilde{v}}{dt} - \frac{N-1}{\rho(x)} q_r - \varepsilon^{\beta-1}. \tag{2.22}$$

Moreover $\rho(x) \ge \rho_1(t) - \frac{3}{2}\varepsilon^{\beta} \ge \frac{3}{2}\varepsilon^{\beta}$ where we have used the definition of T_{ε} for the second inequality. In particular we deduce from (2.22) that for $\varepsilon_3 > 0$ sufficiently small and $\varepsilon \in (0, \varepsilon_3]$,

$$\mathcal{L}[\Phi_{x_0,\rho_0}^{\varepsilon}] \le C_0 + \frac{2}{3}C_0(N-1)\varepsilon^{-\beta} - \varepsilon^{\beta-1} \le 0 \quad \text{for } t \in [0,T_{\varepsilon}],$$

where we used $0 < \beta < \frac{1}{2}$ to deduce the final inequality.

Case 2. $\rho(x) - \rho_1(t) \le -2\varepsilon^{\beta}$: In this case $w(x, t) \equiv -\varepsilon^{\beta}$ is a constant so we have

$$\mathcal{L}[\Phi_{x_0,\rho_0}^{\varepsilon}] = q_v \frac{d\tilde{v}}{dt} + \varepsilon^{-1} q_r \alpha + \varepsilon^{-1} q_{rr} - \varepsilon^{\beta - 1}. \tag{2.23}$$

For sufficiently small $\varepsilon > 0$ we have $|r| = |\varepsilon^{-1}w(x, t)| = |\varepsilon^{\beta - 1}| \ge r_0$ so that (2.18)

$$\left| \varepsilon^{-1} q_r \alpha \right| + \left| \varepsilon^{-1} q_{rr} \right| \le \varepsilon^{-1} (C_0 + 1) e^{-\nu \varepsilon^{\beta - 1}},$$

where the last inequality follows from the choice of $0 < \beta < 1/2$. We can then deduce from (2.23) that

$$\mathcal{L}[\Phi_{x_0,\rho_0}^{\varepsilon}] \le C_0 + \varepsilon^{-1}(C_0 + 1)e^{-\nu\varepsilon^{\beta-1}} - \varepsilon^{\beta-1} \le 0,$$

for $\varepsilon \in (0, \varepsilon_3]$, provided ε_3 is sufficiently small.

Case 3. $-2\varepsilon^{\beta} < \rho(x) - \rho_1(t) < -\frac{3}{2}\varepsilon^{\beta}$: In this case from the definition of w(x,t) we deduce that $w(x,t) \le -\frac{1}{2}\varepsilon^{\beta}$. Choosing $\varepsilon > 0$ sufficiently small so that $|r| = |\varepsilon^{-1}w(x,t)| \ge \frac{1}{2}\varepsilon^{\beta-1} \ge r_0$ we deduce from (2.18) that $|q_r| + |q_{rr}| \le 2e^{-\frac{1}{2}v\varepsilon^{\beta-1}}$. On the other hand we also have that $\rho(x) > \rho_1(t) - 2\varepsilon^{\beta} > \varepsilon^{\beta}$ where the final inequality follows from the definition of T_{ε} . Putting these together into (2.21) we obtain that

$$\mathcal{L}[\Phi_{x_0,\rho_0}^{\varepsilon}] = C_0 + \varepsilon^{-1} e^{-\frac{1}{2}\nu\varepsilon^{\beta-1}} - \varepsilon^{\beta-1} \le 0,$$

for $\varepsilon \in (0, \varepsilon_3]$, where the last inequality again follows from the choice of $0 < \beta < 1/2$ and ε_3 to be sufficiently small.

Choosing $\varepsilon > 0$ to be sufficiently small so that Cases 1–3 hold we thus deduce (2.17a). Finally, the boundary condition (2.17b) follows from $\partial_n \Phi_{x_0,\rho_0}^{\varepsilon}(x,t) = \rho^{-1}\partial_\rho \Phi_{x_0,\rho_0}^{\varepsilon}(x,t)(x-x_0) \cdot n \leq 0$ where the inequality follows from the convexity of Ω and because $\Phi_{x_0,\rho_0}^{\varepsilon}$ is decreasing radially from $x_0 \in \Omega$.

An analogous argument also yields the following result.



72 Page 20 of 31 D. Gomez et al.

Lemma 2.3 Let $\beta \in (0, 1/2)$, $\rho_0 > 0$, T > 0, and $\tilde{v} \in C^1([0, T])$, and $x_0 \in \Omega$ be given. Then there exists $\varepsilon_3 > 0$ small such that for $\varepsilon \in (0, \varepsilon_3]$, the function $\hat{\Phi}^{\varepsilon}_{x_0, \rho_0}$ defined in (2.16) above satisfies

$$\begin{cases}
\partial_{t} \hat{\Phi}_{x_{0},\rho_{0}}^{\varepsilon} - \varepsilon \Delta \hat{\Phi}_{x_{0},\rho_{0}}^{\varepsilon} - \varepsilon^{-1} f(\hat{\Phi}_{x_{0},\rho_{0}}^{\varepsilon}, \tilde{v}(t)) \geq 0 & \text{in } \Omega \times [0, \hat{T}_{\varepsilon}], \\
\partial_{n} \hat{\Phi}_{x_{0},\rho_{0}}^{\varepsilon} \geq 0 & \text{on } \partial \Omega \times [0, \hat{T}_{\varepsilon}].
\end{cases}$$
(2.24)

The following result is an immediate consequence of the comparison principle.

Corollary 2.1 Fix $\beta \in (0, \frac{1}{2})$, T > 0, $\tilde{v} \in C^1([0, T])$, and $x_0 \in \Omega_0$. There exists $\varepsilon_4 \in (0, \varepsilon_3]$ such that if

$$\tilde{u}_0 \ge h^+(\tilde{v}(0); \varepsilon^{\beta})$$
 in $B(x_0, \rho_0) \cap \Omega$, and $\tilde{u}_0 \ge h^-(\tilde{v}(0); 0)$ in $\Omega \backslash B(x_0, \rho_0)$, (2.26)

for some $\rho_0 \ge 4\varepsilon^{\beta}$ and $\varepsilon \in (0, \varepsilon_4]$, then there exists a $\bar{K}_4 > 0$ independent of x_0 such that

$$\tilde{u}^{\varepsilon}(x,t) \ge h^{+}(\tilde{v}(t);0) - \bar{K}_{4}\varepsilon^{\beta}, \quad (x,t) \in B(x_{0},\rho_{0} + \int_{0}^{t} \alpha(\tilde{v}(\tau)) d\tau - (\bar{K}_{4} + 2)\varepsilon^{\beta})$$

$$\times [0,T_{\varepsilon}], \qquad (2.27)$$

where T_{ε} is given by (2.11).

Proof of Corollary 2.1 Let $\Phi_{x_0,\rho_0}^{\varepsilon}(x,t)$ be given by (2.15). By Lemma 2.2 it follows that $\mathcal{L}[\Phi_{x_0,\rho_0}^{\varepsilon}] \leq 0$ in $\Omega \times [0,T_{\varepsilon}]$, and $\partial_n \Phi_{x_0,\rho_0}^{\varepsilon} \leq 0$ on $\partial \Omega \times [0,T_{\varepsilon}]$. Note that $T_{\varepsilon} > 0$ since $\rho_0 > 4\varepsilon^{\beta}$.

To apply the comparison principle, it remains to show that

$$\tilde{u}_0 \ge \Phi_{\mathbf{r}_0, \rho_0}^{\varepsilon}(\cdot, 0) \quad \text{in } \Omega.$$
 (2.28)

We have, on the one hand

$$\tilde{u}_0(x) \ge h^+(\tilde{v}(0); \varepsilon^\beta) \ge \sup_{r \in \mathbb{R}} q(r, \tilde{v}(0); \varepsilon^\beta) \ge \Phi^{\varepsilon}_{x_0, \rho_0}(x, 0) \quad \text{for } x \in B(x_0, \rho_0).$$

On the other hand, we have $w(x, 0) \ge \varepsilon^{\beta}$ in $\Omega \setminus B(x_0, \rho_0)$ so that

$$\Phi_{x_0,\rho_0}^{\varepsilon}(x,0) \le q(\varepsilon^{\beta-1},\tilde{v}(0);\varepsilon^{\beta}) = h^{-}(\tilde{v}(0);\varepsilon^{\beta}) + O(e^{-v\varepsilon^{\beta-1}}) \quad \text{in } \Omega \setminus B(x_0,\rho_0).$$

Now, because $A^- = \inf_{v \in [v_{\min}, v_{\max}]} \frac{d}{da} h^-(v; a)|_{a=0} < 0$ (see Remark 1.1), we deduce that

$$\Phi_{r_0, q_0}^{\varepsilon}(x, 0) \le h^{-}(\tilde{v}(0); 0) + A^{-}\varepsilon^{\beta} + O(\varepsilon^{2\beta})$$



$$+O(e^{-v\varepsilon^{\beta-1}}) \le h^-(\tilde{v}(0);0) \le \tilde{u}_0(x) \quad \text{in } \Omega \backslash B(x_0,\rho_0),$$

for $\varepsilon \in (0, \varepsilon_4]$, with ε_4 sufficiently small and where we have used $\beta \in (0, 1/2)$ in the second inequality. This proves (2.28). Having verified the initial conditions, we can apply the comparison principle to deduce that $\tilde{u}^{\varepsilon}(x, t) \geq \Phi^{\varepsilon}_{x_0, \rho_0}(x, t)$ in $\Omega \times [0, T_{\varepsilon}]$.

To prove (2.27) we first note that for $\varepsilon > 0$ sufficiently small

$$\int_0^t \alpha(\tilde{v}(\tau); \varepsilon^{\beta}) d\tau - 2\varepsilon^{\beta} \ge \int_0^t \alpha(\tilde{v}(\tau)) d\tau - (\bar{K}_4 + 2)\varepsilon^{\beta} \quad \text{for } t \in [0, T_{\varepsilon}],$$

in which we choose any $\bar{K}_4 \geq TA$ where A>0 is the Lipschitz constant of $\alpha(v,a)$ in a. Hence

$$B\left(x_0,\rho_0+\int_0^t\alpha(\tilde{v}(\tau))\,d\tau-(\bar{K}_4+2)\varepsilon^\beta\right)\subset B\left(x_0,\rho_0+\int_0^t\alpha(\tilde{v}(\tau);\varepsilon^\beta)\,d\tau-2\varepsilon^\beta\right).$$

This implies that for any $x \in B(x_0, \rho_0 + \int_0^t \alpha(\tilde{v}(\tau)) d\tau - (\bar{K}_4 + 2)\varepsilon^{\beta})$ we have $w(x, t) \le -\varepsilon^{\beta}$ and in particular

$$\begin{split} \tilde{u}^{\varepsilon}(x,t) &\geq q(-\varepsilon^{\beta-1},\tilde{v}(t);\varepsilon^{\beta}) \geq h^{+}(\tilde{v}(t);\varepsilon^{\beta}) + O(e^{-v\varepsilon^{\beta-1}}) \\ &= h^{+}(\tilde{v}(t);0) + A^{+}\varepsilon^{\beta} + O(\varepsilon^{2\beta}) + O(e^{-v\varepsilon^{\beta-1}}), \end{split}$$

where $A^+ = \inf_{v \in (v_{\min}, v_{\max})} \frac{d}{da} h^+(v; a)|_{a=0} < 0$. Increasing \bar{K}_4 if necessary so that $\bar{K}_4 > |A^+|$ and further reducing $\varepsilon_4 > 0$ then proves (2.27).

Proposition 2.1 Let $0 < \sigma < \beta < \frac{1}{2}$ and T > 0 be fixed. Then there exists an $\varepsilon_5 > 0$ such that for all $\varepsilon \in (0, \varepsilon_1]$

$$\inf_{\tilde{\Omega}_{\varepsilon,\sigma}^{+}(t)} \left(\tilde{u}^{\varepsilon}(\cdot,t) - h^{+}(\tilde{v}(t);0) \right) \ge -\bar{K}_{4}\varepsilon^{\beta} \quad \text{for } t \in [0,T], \tag{2.29}$$

$$\sup_{\tilde{\Omega}_{\varepsilon,\sigma}^{-}(t)} \left(\tilde{u}^{\varepsilon}(\cdot,t) - h^{-}(\tilde{v}(t);0) \right) \leq \bar{K}_{4}\varepsilon^{\beta} \quad for \ t \in [0,T], \tag{2.30}$$

where $\tilde{\Omega}_{\varepsilon,\sigma}^{\pm}(t)$ are given in (2.3) and (2.4).

Proof We will only prove (2.29) since the proof of (2.30) following analogously. We assume, in addition, that $\int_0^t \alpha(\tilde{v}(\tau))d\tau$ does not change sign for $t \in [0, T]$. With some minor modifications, the same proof can be extended to the case where $\int_0^t \alpha(\tilde{v}(\tau))d\tau$ changes sign finitely many times. In light of Lemma 1.3 the assumption that $\int_0^t \alpha(\tilde{v}(\tau))d\tau$ does not change sign is enough for our purpose.

In view of Corollary 2.1 it suffices to show that

$$\tilde{\Omega}_{\varepsilon,\sigma}^{+}(t) \subset \bigcup B\left(x_0, \rho_0(x_0) + \int_0^t \alpha(\tilde{v}(\tau)) d\tau - (\bar{K}_4 + 2)\varepsilon^{\beta}\right)$$
 (2.31)



where $\rho_0(x_0) = \max\{\rho > 0 \mid B(x_0, \rho) \subset \Omega_0\}$ and the union is taken over all $x_0 \in \Omega_0$ such that

$$\rho_0(x_0) \ge \overline{\rho} \varepsilon^{\beta}, \quad \text{where } \overline{\rho} = \max\{4, \overline{K}_4 + 2\}.$$

The proof is divided into two cases depending on whether $\int_0^t \alpha(\tilde{v}(\tau))d\tau$ is nonnegative or nonpositive which corresponds, respectively, to an expanding or contracting activated region.

Case 1. $\int_0^t \alpha(\tilde{v}(\tau)) d\tau \ge 0$ for $t \in [0, T]$: To prove (2.31), we first deduce, by the positivity of $\int_0^t \alpha(\tilde{v}(\tau)) d\tau$ and the definition of T_{ε} , that $T_{\varepsilon} = T$ for all $(x_0, \rho_0(x_0))$ appearing in the union in (2.31). Now, choose any $t_1 \in [0, T]$ and let $x_1 \in \tilde{\Omega}_{\varepsilon, \sigma}^+(t_1)$ and note that by definition this implies $\operatorname{dist}(x_1, \Gamma_0) < \int_0^{t_1} \alpha(\tilde{v}(\tau)) d\tau - \varepsilon^{\sigma}$. We have to consider three subcases depending on the range of $\operatorname{dist}(x_1, \Gamma_0)$.

Case 1a. If $\operatorname{dist}(x_1, \Gamma_0) \leq -\overline{\rho}\varepsilon^{\beta}$ then we can simply choose $x_0 = x_1$ for which we clearly have $\rho_0(x_0) \geq \overline{\rho}\varepsilon^{\beta}$ and $x_1 \in B(x_0, \rho_0(x_0) + \int_0^{t_1} \alpha(\tilde{v}(\tau))d\tau - (\bar{K}_4 + 2)\varepsilon^{\beta})$.

Case 1b. On the other hand if $\operatorname{dist}(x_1, \Gamma_0) \geq 0$ then choose $x' \in \Gamma_0$ such that $|x_1 - x'| = \operatorname{dist}(x_1, \Gamma_0)$. By Lemma 1.2 there exists an $x_0 \in \Omega_0$ such that $B(x_0, \overline{\rho} \varepsilon^{\beta}) \subset \Omega_0$ and $|x_0 - x'| \leq \overline{K_0 \overline{\rho}} \varepsilon^{\beta}$. In particular, $\rho_0(x_0) \geq \overline{\rho} \varepsilon^{\beta}$. By the triangle inequality we then have, for $\varepsilon \in (0, \varepsilon_5]$,

$$\begin{split} |x_1 - x_0| &\leq |x_0 - x'| + |x_1 - x'| \leq \bar{K}_0 \overline{\rho} \varepsilon^{\beta} + \int_0^{t_1} \alpha(\tilde{v}(\tau)) d\tau - \varepsilon^{\sigma} \\ &\leq \rho_0(x_0) + \int_0^{t_1} \alpha(\tilde{v}(\tau)) d\tau - (\bar{K}_4 + 2) \varepsilon^{\beta}, \end{split}$$

where the final inequality follows provided ε_5 is chosen sufficiently small so that $\varepsilon_5 \leq [(\bar{K}_0 - 1)\bar{\rho} + \bar{K}_4 + 2]^{-1/(\beta - \sigma)}$ which we remark, importantly, is independent of x_0 .

Case 1c. Finally, if $-\overline{\rho}\varepsilon^{\beta} < \operatorname{dist}(x_1, \Gamma_0) < 0$ then for $\varepsilon \in (0, \varepsilon_5]$,

$$\overline{\rho}\varepsilon^{\beta} + \int_{0}^{t_{1}} \alpha(\tilde{v}(\tau))d\tau \ge -\operatorname{dist}(x_{1}, \Gamma_{0}) + \int_{0}^{t_{1}} \alpha(\tilde{v}(\tau))d\tau > \varepsilon^{\sigma} > (\bar{K}_{0} + \bar{K}_{4} + 3)\varepsilon^{\beta},$$
(2.32)

where the first strict inequality follows from the definition of $\tilde{\Omega}_{\varepsilon,\sigma}^+(t_1)$ and the second by assuming $\varepsilon_5 \leq [(\bar{K}_0+1)\overline{\rho}+\bar{K}_4+2]^{-1/(\beta-\sigma)}$. We then choose $x'\in\Gamma_0$ such that $|x_1-x'|=\overline{\rho}\varepsilon^\beta$ and using Lemma 1.2 we obtain an $x_0\in\Omega_0$ such that $B(x_0,\overline{\rho}\varepsilon^\beta)\subset\Omega_0$ and $|x_0-x'|\leq \overline{K}_0\overline{\rho}\varepsilon^\beta$. As above we may assume that in fact $\rho_0(x_0)=\overline{\rho}\varepsilon^\beta$. By the triangle inequality and (2.32) above we deduce

$$|x_1 - x_0| \le |x_0 - x'| + |x_1 - x'| \le (1 + \bar{K}_0)\overline{\rho}\varepsilon^{\beta} \le \overline{\rho}\varepsilon^{\beta} + \int_0^{t_1} \alpha(\tilde{v}(\tau))d\tau - (\bar{K}_4 + 2)\varepsilon^{\beta}$$

In summary, the inclusion (2.31) holds for all $\varepsilon \in (0, \varepsilon_5]$ where $\varepsilon_5 = [(K_0 + 1)\overline{\rho} + \overline{K}_4 + 2]^{-1/(\beta - \sigma)}$.



Case 2. $\int_0^t \alpha(v(\tau)) d\tau \le 0$ for $t \in [0, T]$: Let $t_1 \in [0, T]$ and $x_1 \in \tilde{\Omega}_{\varepsilon, \sigma}^+(t_1)$ be given. It follows that $x_1 \in \Omega_0$ and moreover letting $x_0 = x_1$ and $\rho_0 = |\operatorname{dist}(x_1, \Gamma_0)|$ we observe from (2.3) that

$$\rho_0 > \varepsilon^{\sigma} - \int_0^{t_1} \alpha(\tilde{v}(\tau)) d\tau. \tag{2.33}$$

In particular, since $\sigma < \beta$, by choosing a sufficiently small value of ε we can guarantee that $\rho_0 \ge \overline{\rho}$.

We claim that it is enough to show that

$$\rho_0 + \int_0^t \alpha(\tilde{v}; \varepsilon^{\beta}) d\tau > (\bar{K}_4 + 2)\varepsilon^{\beta} \quad \text{for } t \in [0, t_1].$$
 (2.34)

Indeed, if we suppose that (2.34) is true for the moment, then $t_1 \geq T_{\varepsilon}$, and

$$x_1 = x_0 \in B\left(x_0, \rho_0(x_0) + \int_0^{t_1} \alpha(\tilde{v}(\tau)) d\tau - (\bar{K}_4 + 2)\varepsilon^{\beta}\right).$$

To show (2.34), observe that for $t \in [0, t_1]$, we have

$$\rho_{0} + \int_{0}^{t} \alpha(\tilde{v}; \varepsilon^{\beta}) d\tau > \int_{0}^{t} [\alpha(\tilde{v}(\tau); \varepsilon^{\beta}) - \alpha(\tilde{v}(\tau))] d\tau + \varepsilon^{\sigma}$$

$$\geq -A\varepsilon^{\beta} T + O(\varepsilon^{2\beta}) + \varepsilon^{\sigma} > (\bar{K}_{4} + 2)\varepsilon^{\beta} \quad \text{for all } t \in [0, t_{1}],$$

where we used (2.33) to get the first inequality, A is the Lipschitz constant of $\alpha(v; a)$ in a, and where $\varepsilon \in (0, \varepsilon_1)$ is chosen to get the final inequality, with $\varepsilon_5 > 0$ being reduced further from Case 1 above if necessary.

Proof of Theorem 3 We again assume that $\int_0^t \alpha(\tilde{v}(\tau)) d\tau$ does not change sign in [0, T]. The global bounds (2.7) are proved in Lemma 2.1 above. To prove (2.5) it therefore suffices to show there exist $\bar{K}_2 > 0$ so that

$$\tilde{u}^{\varepsilon}(x,t) \ge h^{+}(\tilde{v}(t)) - \bar{K}_{2}\varepsilon^{\beta} \quad \text{for } (x,t) \in \tilde{\Omega}^{+}_{\varepsilon,\sigma,T},$$
 (2.35)

and

$$\tilde{u}^{\varepsilon}(x,t) \le h^{-}(\tilde{v}(t)) + \bar{K}_{2}\varepsilon^{\beta} \quad \text{for } (x,t) \in \tilde{\Omega}_{\varepsilon,\sigma,T}^{-}.$$
 (2.36)

These are direct consequences of Proposition 2.1. This completes the proof of Theorem 3.

3 Proof of Theorem 2

Having established Theorem 3 in Sect. 2 above we turn now to the proof of Theorem 2. Let T > 0 and $\gamma \in (0, 1/2)$ be given, and fix β , σ such that $0 < \gamma < \sigma < \beta < 1/2$.



72 Page 24 of 31 D. Gomez et al.

In addition, fix

$$B = \frac{8K(A + 2\bar{K}_2\varepsilon_2)^2}{\theta},\tag{3.1}$$

where ε_2 is the (*T*-dependent) constant in Theorem 3, $\theta \in (0, 1)$ is the constant in (1.16) of assumption (A4), A > 0 is the constant in (1.17), and where we define

$$K = \sup_{s \in \mathbb{R}} |\{x \in \Omega \mid \operatorname{dist}(x, \Gamma_0) = s\}|. \tag{3.2}$$

In view of Lemma 1.3 we have $v_{\min} < \hat{v}(t) < v_{\max}$ for all $t \ge 0$ and hence there exists an $0 < \varepsilon_1 \le \min\{\varepsilon_2, \varepsilon_3, \varepsilon_4, \varepsilon_5\}$ such that for all $\varepsilon \in (0, \varepsilon_1]$

$$v_{\min} < \hat{v}(t) \pm \varepsilon^{\gamma} e^{Bt} < v_{\max}$$
 for all $t \in [0, T]$.

Define

$$T(\varepsilon) \equiv \sup\{t \in [0, T] \, \big| \, |v^{\varepsilon}(\tau) - \hat{v}(\tau)| < \varepsilon^{\gamma} e^{B\tau} \quad \text{for all } 0 \le \tau \le t\}. \tag{3.3}$$

and note that $T(\varepsilon) > 0$ for all $\varepsilon \in (0, \varepsilon_1]$ since $v^{\varepsilon}(0) = \hat{v}(0)$. We will show that in fact $T(\varepsilon) = T$.

Let $u_+^{\varepsilon}(x, t)$ be the unique solution of

$$\begin{cases} \partial_t u_{\pm}^{\varepsilon} = \varepsilon \Delta u_{\pm}^{\varepsilon} + \varepsilon^{-1} f(u_{\pm}^{\varepsilon}, \hat{v}(t) \pm \varepsilon^{\gamma} e^{Bt}), & \text{in } \Omega \times (0, T], \\ \partial_n u_{\pm}^{\varepsilon} = 0, & \text{on } \partial\Omega \times (0, T], \\ u_{\pm}^{\varepsilon}(x, 0) = u_0(x), & \text{in } \Omega. \end{cases}$$
(3.4)

For each $t \in [0, T]$, define $\hat{\Omega}_{\varepsilon}^{+}(t)$, $\hat{\Omega}_{\varepsilon}^{-}(t)$, and $\hat{\Omega}_{\varepsilon}^{0}(t)$ by

$$\hat{\Omega}_{\varepsilon,\sigma}^{+}(t) \equiv \{ x \in \Omega \mid \operatorname{dist}(x, \Gamma_0) < \int_0^t \alpha(\hat{v}(\tau) - \varepsilon^{\gamma} e^{B\tau}) d\tau - \varepsilon^{\sigma} \}, \quad \text{for } t \in [0, T],$$
(3.5)

$$\hat{\Omega}_{\varepsilon,\sigma}^{-}(t) \equiv \{ x \in \Omega \mid \operatorname{dist}(x, \Gamma_0) > \int_0^t \alpha(\hat{v}(\tau) + \varepsilon^{\gamma} e^{B\tau}) d\tau + \varepsilon^{\sigma} \}, \quad \text{for } t \in [0, T],$$
(3.6)

$$\hat{\Omega}_{\varepsilon,\sigma}^{0}(t) \equiv \Omega \setminus [\hat{\Omega}_{\varepsilon,\sigma}^{+}(t) \cup \hat{\Omega}_{\varepsilon,\sigma}^{-}(t)], \qquad \text{for } t \in [0, T].$$
(3.7)

We refer the reader to Fig. 8 for an illustration of these three regions. Reducing ε_1 further if needed, we may apply Theorem 3 to u_{\pm}^{ε} to deduce that for all $t \in [0, T]$ and $\varepsilon \in (0, \varepsilon_1]$,

$$\sup_{\hat{\Omega}_{\varepsilon,\sigma}^{+}(t)} |u_{+}^{\varepsilon}(\cdot,t) - h^{+}(\hat{v}(t) + \varepsilon^{\gamma}e^{Bt})| + \sup_{\hat{\Omega}_{\varepsilon,\sigma}^{+}(t)} |u_{-}^{\varepsilon}(\cdot,t) - h^{+}(\hat{v}(t) - \varepsilon^{\gamma}e^{Bt})| \leq \bar{K}_{2}\varepsilon^{\beta}.$$

$$(3.8)$$



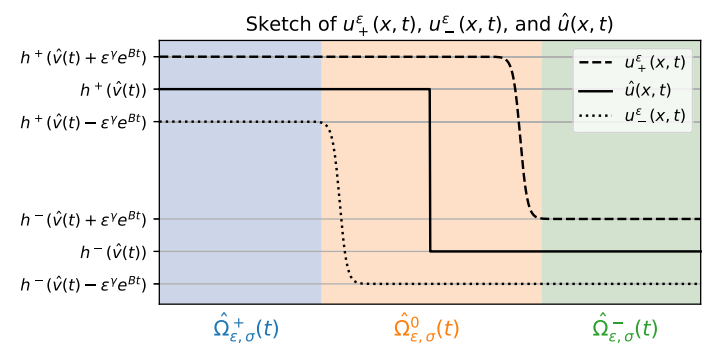


Fig. 8 Sketch of the leading order solution $\hat{u}(x,t)$ given by (1.10c), ε -dependent solutions $u_{\pm}^{\varepsilon}(x,t)$ satisfying (3.4), and the regions $\hat{\Omega}_{\varepsilon,\sigma}^{+}(t)$, $\hat{\Omega}_{\varepsilon,\sigma}^{0}(t)$, and $\hat{\Omega}_{\varepsilon,\sigma}^{-}(t)$ used in the proof of Theorem 2

Next we observe that assumption (A3) and the definition of $T(\varepsilon)$ imply that for all $\varepsilon \in (0, \varepsilon_3]$ and $t \in [0, T_{\varepsilon}]$ we have

$$\begin{cases} f(u_{-}^{\varepsilon}(x,t), v^{\varepsilon}(t)) > f(u_{-}^{\varepsilon}(x,t), \hat{v}(t) - \varepsilon^{\gamma} e^{Bt}), \\ f(u_{+}^{\varepsilon}(x,t), v^{\varepsilon}(t)) < f(u_{+}^{\varepsilon}(x,t), \hat{v}(t) + \varepsilon^{\gamma} e^{Bt}). \end{cases}$$
(3.9)

By regarding $u^{\varepsilon}(x,t)$ as the solution of a single parabolic equation with Neumann boundary conditions (with $v^{\varepsilon}(t)$ being a given parameter), and regarding u^{ε}_{+} , u^{ε}_{-} as the super and subsolution of the same equation (thanks to (3.9)), we may apply the comparison principle to obtain

$$u_{-}^{\varepsilon}(x,t) \leq u^{\varepsilon}(x,t) \leq u_{+}^{\varepsilon}(x,t)$$
 for all $(x,t) \in \Omega \times [0,T(\varepsilon)]$ and $\varepsilon \in (0,\varepsilon_1]$.

(3.10)

The definition of $v^{\varepsilon}(t)$ in (1.1) together with definition (1.10b) of $\hat{v}(t)$ and (1.10c) then imply that for all $\varepsilon \in (0, \varepsilon_1]$ and $t \in [0, T(\varepsilon)]$

$$|v^{\varepsilon}(t) - \hat{v}(t)| = \left| \int_{\Omega} (u^{\varepsilon}(x, t) - \hat{u}(x, t)) \, dx \right|$$

$$\leq \int_{\hat{\Omega}_{\varepsilon, \sigma}^{+}(t)} |u^{\varepsilon} - \hat{u}| \, dx + \int_{\hat{\Omega}_{\varepsilon, \sigma}^{-}(t)} |u^{\varepsilon} - \hat{u}| \, dx + \int_{\hat{\Omega}_{\varepsilon, \sigma}^{0}(t)} |u^{\varepsilon} - \hat{u}| \, dx$$

$$= I_{+} + I_{-} + I_{0}. \tag{3.11}$$

We now estimate each term in (3.11), starting with I_+ . By (3.8) and (3.10) we deduce that for all $\varepsilon \in (0, \varepsilon_1]$ and $t \in [0, T(\varepsilon)]$

$$h^+(\hat{v}(t)-\varepsilon^{\gamma}e^{Bt}) - \bar{K}_2\varepsilon^{\beta} \leq u^{\varepsilon}(x,t) \leq h^+(\hat{v}(t)+\varepsilon^{\gamma}e^{Bt}) + \bar{K}_2\varepsilon^{\beta} \quad \text{for } x \in \hat{\Omega}^+_{\varepsilon,\sigma}(t).$$



72 Page 26 of 31 D. Gomez et al.

Note that $\hat{u}(x,t) = h^+(\hat{v}(t))$ for $x \in \hat{\Omega}_{\varepsilon,\sigma}^+(t)$ since $\hat{\Omega}(t) \subset \hat{\Omega}_{\varepsilon,\sigma}^+(t)$ by Lemma 1.1. In particular

$$\begin{split} \sup_{x \in \hat{\Omega}_{\varepsilon,\sigma}^+(t)} |u^{\varepsilon} - \hat{u}| &\leq \max \left\{ |h^+(\hat{v}(t) - \varepsilon^{\gamma} e^{Bt}) - \bar{K}_2 \varepsilon^{\beta} - h^+(\hat{v}(t))|, |h^+(\hat{v}(t) + \varepsilon^{\gamma} e^{Bt}) + \bar{K}_2 \varepsilon^{\beta} - h^+(\hat{v}(t))| \right\} \\ &\leq (1 - \theta) \varepsilon^{\gamma} e^{Bt} + \bar{K}_2 \varepsilon^{\beta} \quad \text{for } t \in [0, T(\varepsilon)] \text{ and } \varepsilon \in (0, \varepsilon_1], \end{split}$$

where we used (1.16) in assumption (A4). Since $\beta > \gamma > 0$, and possibly reducing ε_1 so that $\varepsilon_1 \leq (\bar{K}_2^{-1}\theta e^{BT}/3)^{\frac{1}{\beta-\gamma}}$, we deduce that for all $\varepsilon \in (0, \varepsilon_1]$ and $t \in [0, T(\varepsilon)]$

$$\sup_{x \in \hat{\Omega}_{\varepsilon,\sigma}^{k}(t)} |u^{\varepsilon}(x,t) - \hat{u}(x,t)| \le \left(1 - \frac{2}{3}\theta\right) \varepsilon^{\gamma} e^{Bt}.$$

In particular, for all $\varepsilon \in (0, \varepsilon_1]$ we have

$$|I_{+}| \le |\hat{\Omega}_{\varepsilon,\sigma}^{+}(t)| \left(1 - \frac{2}{3}\theta\right) \varepsilon^{\gamma} e^{Bt} \quad \text{for } t \in [0, T(\varepsilon)],$$
 (3.12)

and similarly also

$$|I_{-}| \le |\hat{\Omega}_{\varepsilon,\sigma}^{-}(t)| \left(1 - \frac{2}{3}\theta\right) \varepsilon^{\gamma} e^{Bt} \quad \text{for } t \in [0, T(\varepsilon)].$$
 (3.13)

Next we estimate I_0 . To this end we first observe that for $\varepsilon \in (0, \varepsilon_1]$, and $t \in [0, T(\varepsilon)]$ we have

$$\sup_{x \in \Omega} |u^{\varepsilon}(x,t) - \hat{u}^{\varepsilon}(x,t)| \le |h^{+}(\hat{v}(t) + \varepsilon^{\gamma}e^{Bt}) - h^{-}(\hat{v}(t) - \varepsilon^{\gamma}e^{Bt})| + 2\bar{K}_{2}\varepsilon \le A + 2\bar{K}_{2}\varepsilon_{1},$$
(3.14)

where the first inequality follows from (3.10), (2.7), and the triangle inequality while the second inequality follows from (1.17). Moreover, by the definition of Ω_{ε}^{0} we have that

$$\begin{split} |\hat{\Omega}^{0}_{\varepsilon,\sigma}(t)| &\leq K \left[\int_{0}^{t} [\alpha(\hat{v}(\tau) + \varepsilon^{\gamma} e^{B\tau}) - \alpha(\hat{v}(\tau) - \varepsilon^{\gamma} e^{B\tau})] \, d\tau + 2\varepsilon^{\sigma} \right] \\ &\leq K A \int_{0}^{t} 2\varepsilon^{\gamma} e^{B\tau} \, d\tau + 2K\varepsilon^{\sigma} \\ &\leq \frac{\theta}{4(A + 2\bar{K}_{2}\varepsilon_{1})} \varepsilon^{\gamma} e^{Bt} + 2K\varepsilon^{\sigma} \quad \text{for } t \in [0,T] \text{ and } \varepsilon \in (0,\varepsilon_{1}], \end{split}$$

where we used the definition (3.2) of K for the first inequality, the bound (1.17) in the second inequality, and the definition (3.1) of B for the final inequality. Reducing ε_1 further if necessary we deduce that for all $\varepsilon \in (0, \varepsilon_1]$,

$$|\hat{\Omega}_{\varepsilon,\sigma}^{0}(t)| \leq \frac{\theta}{3(A+2\bar{K}_{2}\varepsilon_{1})} \varepsilon^{\gamma} e^{Bt} \quad \text{for } t \in [0, T(\varepsilon)],$$



and in particular

$$|I_{0}| \leq \int_{\hat{\Omega}_{\varepsilon,\sigma}^{0}(t)} |u^{\varepsilon} - \hat{u}| \, dx \leq |\hat{\Omega}_{\varepsilon,\sigma}^{0}(t)| (A + 2\bar{K}_{2}\varepsilon_{1}) \leq \frac{\theta}{3} e^{\gamma} e^{Bt} \quad \text{for } t \in [0, T(\varepsilon)],$$
(3.15)

where we used (3.14) in the second inequality.

Substituting (3.12), (3.13) and (3.15) into (3.11), we deduce that

$$|v^{\varepsilon}(t) - \hat{v}| \le \left(|\Omega|\left(1 - \frac{2}{3}\theta\right) + \frac{\theta}{3}\right)\varepsilon^{\gamma}e^{Bt} \le \left(1 - \frac{1}{3}\theta\right)\varepsilon^{\gamma}e^{Bt} \quad \text{for } t \in [0, T(\varepsilon)],$$
(3.16)

where we used the fact that $|\Omega_{\varepsilon}^+(t)| + |\Omega_{\varepsilon}^-(t)| \leq |\Omega| = 1$. The definition (3.3) of $T(\varepsilon)$, together with (3.16) above, imply that $T(\varepsilon) = T$ for otherwise it would be inconsistent with the maximality of $T(\varepsilon)$. In particular this establishes (1.18a) with $\bar{K}_1 = e^{BT}$. Furthermore, the bounds (3.10) hold for all $t \in [0, T]$ so that applying the global estimate (2.7) of Theorem 3 to $u_+^{\varepsilon}(x, t)$ and $u_-^{\varepsilon}(x, t)$ then yields the global estimate (1.18b).

Finally, we prove (1.19). Using (1.17), and enlarging \bar{K}_1 if necessary, we have

$$\left\{ x \in \Omega \middle| \operatorname{dist}(x, \Gamma_0) < \int_0^t \alpha(\hat{v}(\tau)) d\tau - \bar{K}_1 \varepsilon^{\gamma} \right\} \subset \hat{\Omega}_{\varepsilon, \sigma}^+(t) \quad \text{for all } t \in [0, T], \ \varepsilon \in (0, \varepsilon_1],$$
(3.17)

where we remind the reader that $0 < \gamma < \sigma < \beta < \frac{1}{2}$. By the Lipschitz continuity of $h^+(v)$ and (3.8) we deduce that for all $t \in [0, T]$ and $\varepsilon \in (0, \varepsilon_1]$

$$|u_{+}^{\varepsilon} - h^{+}(\hat{v}(t))| + |u_{-}^{\varepsilon} - h^{+}(\hat{v}(t))| \leq \bar{K}_{1}\varepsilon^{\gamma} \quad \text{when } \operatorname{dist}(x, \Gamma_{0}) < \int_{0}^{t} \alpha(\hat{v}(\tau)) d\tau - \bar{K}_{1}\varepsilon^{\gamma}, \tag{3.18}$$

where we have also used the set inclusion (3.17). Having already established that $T(\varepsilon) = T$ we see that the inequalities in (3.10) hold for $\Omega \times [0, T]$ provided $\varepsilon \in (0, \varepsilon_1]$. Combining (3.10) and (3.18), we therefore deduce that for all $t \in [0, T]$ and $\varepsilon \in (0, \varepsilon_1]$

$$|u^{\varepsilon} - h^{+}(\hat{v}(t))| \leq \bar{K}_{1}\varepsilon^{\gamma}$$
 when $\operatorname{dist}(x, \Gamma_{0}) < \int_{0}^{t} \alpha(\hat{v}(\tau)) d\tau - \bar{K}_{1}\varepsilon^{\gamma}, \ t \in [0, T],$

$$(3.19)$$

which proves the first estimate of (1.19). The second one can be established in an analogous manner and we omit the details.

4 Discussion

In this paper we have initiated a rigorous study of the limiting behaviour of solutions to the non-local problem (1.1) when $\varepsilon \ll 1$. Formal asymptotic calculations suggest



that this system exhibits growing or shrinking activated regions with a common normal velocity α (depending on the level of v(t)) over an O(1) timescale. For spatial dimension $N \geq 2$, it is expected that, over a slower $O(\varepsilon^{-1})$ timescale, higher order effects lead to a volume-preserving mean curvature flow (see Fig. 6) that possibly interacts with the boundary $\partial \Omega$; see (Chen et al. 2010) for a discussion on volume-preserving mean curvature flow in the volume-preserving Allen-Cahn equation, as well as (Mugnai et al. 2016) and the references therein for the mathematical aspects of volume-preserving mean curvature flow. In this paper we have focused on the leading order dynamics over an O(1) timescale. Specifically, in Theorem 2, we have shown that for any T>0 and $\gamma\in(0,1/2)$ the values of $u^\varepsilon(x,t)$ and $v^\varepsilon(t)$ are within $O(\varepsilon^\gamma)$ of those predicted by the formal asymptotics for all $t\in[0,T]$ and $x\in\Omega$ outside of an $O(\varepsilon^\gamma)$ boundary layer near the interface between activated and inactivated regions. In particular, these quantitative results rigorously locate the front interface within $O(\varepsilon^\gamma)$. These results also rigorously justify the wave-pinning behaviour previously predicted by formal asymptotics and numerical simulations.

One of the key steps in the proof of Theorem 2 was the construction of two bounding solutions $u_{\pm}^{\varepsilon}(x,t)$ satisfying the *scalar* equation (2.1). For a bistable potential that is independent of (x,t), Chen (1992) proved the generation of interface and the motion by normal velocity via super/subsolution method. On the other hand for a bistable potential with (x,t) dependence, the limiting behavior of solutions has been previously established in Barles et al. (1993) using viscosity solutions methods; see also (Alfaro et al. 2008). Our contribution in Sect. 2 is to obtain a quantitative estimate of the transition between the two stable states within $O(\varepsilon^{\gamma})$ distance of the limiting interface when $\varepsilon \to 0$.

An interesting feature of (1.1) is that the leading order interface may potentially lose regularity by forming cusps, even if the initial interface is smooth. This happens when the interface touches the boundary or when the curvature of the interface blows up at an interior point. In such a case the error of order ε^{γ} with $\gamma \in (0, 1/2)$ seems to be sharp. Here we refer to Fig. 5c, which measures roughly the maximum distance d_{max} of the reaction–diffusion interface with the one predicted by the leading order theory. For t = 0.2, 0.5, 1 the leading order interface is regular and $d_{\text{max}} = O(\varepsilon)$, whereas for t = 2, 5 the leading order interface has a cusp and d_{max} is of fractional order in ε .

Next, we discuss the assumption on the initial data to be of bang-bang type for our results. For Theorem 3 it is possible to relax the initial data to $\tilde{u}_0 \in C^1(\overline{\Omega})$ and

$$|\nabla_x \tilde{u}_0| > 0$$
 when $\tilde{u}_0 = h^0(\tilde{v}(0))$.

In this case, one can define $\Gamma_0 = \{x \in \Omega \mid \tilde{u}_0(x) = h^0(\tilde{v}(0))\}$, and follow the arguments in Chen (1992) to prove the generation of interface. For Theorem 2 concerning the nonlocal equation (1.1), however, the situation is more complicated. Although one might also expect the generation of interface to be valid, it is not clear in general how to characterize the exact initial location of the generated interface in terms of the initial data $u_0(x)$ and $v(0) = M_0 - \frac{1}{|\Omega|} \int_{\Omega} u_0(x) \, dx$. This is the main reason we required that the initial data being of bang-bang type in Theorem 2.



In contrast, the assumption (A5) on the domain convexity is not necessary. In fact, our arguments can be adapted to treat nonconvex domains with C^2 boundary. This can be done by enforcing an upper bound on the radius of the super/subsolutions constructed in Sect. 1.5. Finally we conclude by drawing attention to assumption (A4) that is necessary for proving Theorem 2 but is not necessary for wave-pinning. We suggest the weakening of this assumption as a further open problem for which different techniques than those used in this paper may be needed.

Acknowledgements D. Gomez is supported by NSERC and the Simons Foundation. K.-Y. Lam is supported by the National Science Foundation and European Research Council (ERC) under the European Union's Horizon 2020 research and innovation programme (grant agreement No 740623). Y. Mori is supported by the Simons Foundation. The support of the Institut Henri Poincaré (UAR 839 CNRS-Sorbonne Université) and LabEx CARMIN (ANR-10-LABX-59-01) is also acknowledged.

Appendix A. The differential algebraic equation and its solvability

In this appendix we reformulate the system (1.10) as a differential algebraic equation (DAE) that more easily lends itself to numerical calculations and analysis. To this end we first define

$$W(s) \equiv |\{x \in \Omega \mid \operatorname{dist}(x, \Gamma_0) < s\}|.$$

Since s is the distance of the interface from its initial position, it is easy to see that ds/dt indicates its speed which, by the method of matched asymptotic expansions, corresponds to α . Specifically, we deduce that (1.10) is equivalent to the system

$$\frac{ds}{dt} = \alpha(V(s)), t > 0; \quad s(0) = 0,$$
 (A.1a)

$$V(s) + W(s)h^{+}(V(s)) + (1 - W(s))h^{-}(V(s)) = M_{0}.$$
 (A.1b)

It is then straightforward to recover $\hat{v}(t)$ and $\hat{\Omega}(t)$ by using

$$\hat{v}(t) = V(s(t)), \quad \hat{\Omega}(t) = \{ x \in \Omega | \operatorname{dist}(x, \Gamma_0) < s(t) \},$$

from which $\hat{u}(x,t)$ is then obtained using (1.10c). While solving the DAE (A.1) is a relatively simple task, the calculation of W(s) may be more difficult depending on properties of the initial interface Γ_0 . However, this reformulation has the benefit that once the initial interface Γ_0 is known, W(s) can be precomputed for a sufficiently large range of s values.

In addition to simplifying numerical calculation of the leading order solution, it is also easier to deduce the existence of solutions to (A.1). It suffice to show that the right hand side of (A.1a) is Lipschitz in s. To show this we first define G: $(v_{\min}, v_{\max}) \times (0, 1) \to \mathbb{R}$ by

$$G(x, y) \equiv x + yh^{+}(x) + (1 - y)h^{-}(x) = y(h^{+}(x) + x) + (1 - y)(h^{-}(x) + x)$$



72 Page 30 of 31 D. Gomez et al.

Then for $x_2 > x_1$ we calculate

$$G(x_2, y) - G(x_1, y) = y(x_2 - x_1) \int_0^1 \left(1 + \frac{dh^+}{dv} |_{sx_2 + (1-s)x_1} \right) ds$$

$$+ (1 - y)(x_2 - x_1) \int_0^1 \left(1 + \frac{dh^-}{dv} |_{sx_2 + (1-s)x_1} \right) ds$$

$$> C_0 y(x_2 - x_1) + C_0 (1 - y)(x_2 - x_1) = C_0 (x_2 - x_1),$$

where the first inequality follows from (1.12) and in particular $dh^{\pm}/dv > -1$. On the other hand

$$G(x, y_2) - G(x, y_1) \le |h^+(x) - h^-(x)||y_2 - y_1| \le A|y_2 - y_1|.$$

Now let s_1 and s_2 satisfy (A.1b) and assume that $V(s_2) > V(s_1)$. Then

$$G(V(s_2), W(s_1)) - G(V(s_1), W(s_1)) = G(V(s_2), W(s_1)) - G(V(s_2), W(s_2)),$$

with which the above inequalities give

$$C_0|V(s_2) - V(s_1)| < A|W(s_2) - W(s_1)|.$$
 (A.2)

Now from the definition of W(s) we deduce $|W(s_2) - W(s_1)| < C_1|s_2 - s_1|$ for some constant $C_1 > 0$ depending only on Γ_0 . From (1.17) we then deduce

$$|\alpha(V(s_2)) - \alpha(V(s_1))| \le A|V(s_2) - V(s_1)| \le \frac{A^2C_1}{C_0}|s_2 - s_1|.$$
 (A.3)

References

Alfaro M, Hilhorst D, Matano H (2008) The singular limit of the Allen–Cahn equation and the FitzHugh–Nagumo system. J Differ Equ 245(2):505–565

Barles G, Bronsard L, Souganidis PE (1992) Front propagation for reaction–diffusion equations of bistable type. Ann Inst H Poincaré C Anal Non Linéaire 9(5):479–496

Barles G, Soner HM, Souganidis PE (1993) Front propagation and phase field theory. SIAM J Control Optim 31(2):439–469

Champneys AR, Al Saadi F, Breña-Medina VF, Grieneisen VA, Marée AF, Verschueren N, Wuyts B (2021) Bistability, wave pinning and localisation in natural reaction—diffusion systems. Phys D 416:132735

Chen X (1992) Generation and propagation of interfaces for reaction–diffusion equations. J Differ Equ 96(1):116-141

Chen X, Hilhorst D, Logak E (2010) Mass conserving Allen–Cahn equation and volume preserving mean curvature flow. Interfaces Free Bound 12(4):527–549

Cusseddu D, Edelstein-Keshet L, Mackenzie JA, Portet S, Madzvamuse A (2019) A coupled bulk-surface model for cell polarisation. J Theor Biol 481:119–135

Diegmiller R, Montanelli H, Muratov CB, Shvartsman SY (2018) Spherical caps in cell polarization. Biophys J 115(1):26–30

Fife PC, McLeod JB (1977) The approach of solutions of nonlinear diffusion equations to travelling front solutions. Arch Ration Mech Anal 65(4):335–361

Giese W, Eigel M, Westerheide S, Engwer C, Klipp E (2015) Influence of cell shape, inhomogeneities and diffusion barriers in cell polarization models. Phys Biol 12(6):066014



Goryachev AB, Leda M (2017) Many roads to symmetry breaking: molecular mechanisms and theoretical models of yeast cell polarity. Mol Biol Cell 28(3):370–380

Jilkine A, Edelstein-Keshet L (2011) A comparison of mathematical models for polarization of single eukaryotic cells in response to guided cues. PLoS Comput Biol 7(4):e1001121

Lam K-Y, Lou Y (2022) Introduction to reaction—diffusion equations: theory and applications to spatial ecology and evolutionary biology. Lecture notes on mathematical modelling in the life sciences. Springer, Cham

Lunardi A (1995) Analytic semigroups and optimal regularity in parabolic problems. Modern Birkhäuser classics. Birkhäuser, Basel [2013 reprint of the 1995 original] [MR1329547]

Mori Y, Jilkine A, Edelstein-Keshet L (2008) Wave-pinning and cell polarity from a bistable reaction–diffusion system. Biophys J 94(9):3684–3697

Mori Y, Jilkine A, Edelstein-Keshet L (2011) Asymptotic and bifurcation analysis of wave-pinning in a reaction-diffusion model for cell polarization. SIAM J Appl Math 71(4):1401-1427

Mugnai L, Seis C, Spadaro E (2016) Global solutions to the volume-preserving mean-curvature flow. Calc Var Partial Differ Equ 55(1):Art. 18, 23

PDE Solutions Inc. Flexpde 7. http://www.pdesolutions.com

Rappel W-J, Edelstein-Keshet L (2017) Mechanisms of cell polarization. Curr Opin Syst Biol 3:43-53

Rätz A, Röger M (2012) Turing instabilities in a mathematical model for signaling networks. J Math Biol 65(6):1215–1244

Rubinstein J, Sternberg P (1992) Nonlocal reaction–diffusion equations and nucleation. IMA J Appl Math 48(3):249–264

Zmurchok C, Collette J, Rajagopal V, Holmes WR (2020) Membrane tension can enhance adaptation to maintain polarity of migrating cells. Biophys J 119(8):1617–1629

Publisher's Note Springer Nature remains neutral with regard to jurisdictional claims in published maps and institutional affiliations.

Springer Nature or its licensor (e.g. a society or other partner) holds exclusive rights to this article under a publishing agreement with the author(s) or other rightsholder(s); author self-archiving of the accepted manuscript version of this article is solely governed by the terms of such publishing agreement and applicable law.

